THE DETERMINATION OF THE GEOMETRIES OF MULTIPLE-ELEMENT AIRFOILS OPTIMIZED FOR MAXIMUM LIFT COEFFICIENT

BY

ALLEN WEN-SHIN CHEN
B.S.E., National Taiwan University, 1965
M.S., University of Illinois, 1969

THESIS

Submitted in partial fulfillment of the requirements
for the degree of Doctor of Philosophy in Aeronautical and Astronautical Engineering
in the Graduate College of the
University of Illinois at Urbana-Champaign, 1971

Urbana, Illinois

THE DETERMINATION OF THE GEOMETRIES OF MULTIPLE-ELEMENT AIRFOILS OPTIMIZED FOR MAXIMUM LIFT COEFFICIENT

Allen Wen-shin Chen, Ph.D.
Department of Aeronautical and Astronautical Engineering
University of Illinois at Urbana-Champaign, 1971

Optimum airfoils in the sense of maximum lift coefficient are obtained by a newly developed method. The maximum lift coefficient is achieved by requiring that the turbulent skin friction be zero in the pressure rise region on the upper surface. Under this constraint, the pressure distribution is optimized. The optimum pressure distribution consists of a uniform stagnation pressure on the lower surface, a uniform minimum pressure on the upper surface immediately downstream of the front stagnation point followed by a Stratford zero skin friction pressure rise. When multiple-element airfoils are under consideration, this optimum pressure distribution appears on every element. The parameters used to specify the pressure distribution on each element are the Reynolds number Re_0 and the normalized trailing edge velocity q_U.

The newly developed method of design computes the velocity distribution on a given airfoil and modifies the airfoil contour in a systematic manner until the desired velocity distribution is achieved. There are no limitations on how many elements the airfoil to be designed can have. Numerical examples of one- and two-element airfoils are given. The $C_{L_{max}}$ values obtained range from 2 to 2.5.

To my parents

ACKNOWLEDGMENT

The author wishes to express his sincere appreciation to Professor Allen I. Ormsbee for suggesting this problem and for his advice during the course of this study. The author is also grateful for the Langley Research Center of the National Aeronautical and Space Administration for their financial support of this study under the contract NGR 14-005-144. Special thanks are due to the author's wife, Judy. This work could not have been accomplished without her confidence and encouragement.

TABLE OF CONTENTS

I. INTRODUCTION

Airfoils with high maximum lift coefficient ($C_{L_{max}}$) are desirable for certain types of aircraft. With their large $C_{L_{max}}$, these airfoils can be operated at a comparatively low speed while producing a large amount of lift force. This characteristic is of primary interest in the design of aircraft with short take-off and landing run capability.

Since the value of $C_{L_{max}}$ is limited by the occurrence of boundary layer separation on the upper surface of an airfoil where the fluid is subject to an adverse pressure gradient, the approach to obtaining a high-lift airfoil is to delay or entirely suppress the flow separation. In 1920, Lachmann and Handley-Page designed the first high-lift wing which consisted of a conventional airfoil and a small additional element called a leading edge slat. This leading edge slat gives the fluid which passes through the gap between the slat and the main airfoil a high velocity. Consequently, the boundary layer which grows on the upper surface of the main airfoil has more momentum than it would have in the absence of the slat. This high-momentum boundary layer can sustain a steeper adverse pressure gradient and hence delay the separation. Therefore, by placing the leading edge slat at an appropriate position, the airfoil can be operated at a higher angle of attack without flow separation and the lift force is increased. An alternative way of obtaining more lift force is to put an additional element near the trailing edge of the airfoil. The so-called trailing edge flap does not delay the separation of boundary layer on the upper surface of the airfoil. It produces additional circulation and hence lift force by both its presence and the velocity

it induces on the main airfoil. Performance of airfoils which have leading edge slats and/or trailing edge flaps are available in the literature. With all these auxiliary elements to provide more lift force for a given airfoil, few attempts have been made to find the maximum lift coefficient which can be obtained on a single element airfoil. The first successful work in this area was accomplished by Liebeck and Ormsbee.[1] They designed a series of airfoils possessing large values of $C_{L_{max}}$ by requiring the pressure on the upper surface of an airfoil to rise in such a way that the turbulent skin friction is zero whatever the pressure is increasing. These airfoils are optimum in the sense of maximum lift coefficient. Zero skin-friction means that the boundary layer is about to separate. Thus, any attempts to obtain a larger lift coefficient by either increasing peak velocity or shifting the point of peak velocity in the downstream direction will result in a flow separation. With this zero skin-friction requirement, a variational problem was set up in order to find the pressure distribution which would provide the maximum lift coefficient. The solution to this variational problem specified the pressure distribution on the upper surface of the airfoil and one of the standard methods of airfoil design was employed to obtain the geometry of the optimum airfoil.

Since more lift can always be obtained by appropriately using a leading edge slat and/or a trailing flap, a natural extension of Liebeck and Ormsbee's work would be the search for optimum multiple-element airfoils in the sense of maximum lift coefficient. This is the goal of this research. The study consists of two parts. The first part deals with the search for pressure distributions which provide a maximum lift coefficient. The second part determines

the geometry of the multiple-element airfoil which produces these pressure distributions. As will be seen in the next chapter, the optimum pressure distribution is found to be identical to the one for single-element airfoils. A new method of two-dimensional airfoil design is developed to obtain the geometries of the airfoils which produce these optimum pressure distributions. Since no methods of multiple-element airfoil design are available in the literature, the method developed in this research may be considered as a major contribution to this aspect of aeronautical science. This method makes it possible to obtain the geometries of each element of the multiple-element airfoil when the pressure distribution is specified along the surface of each element. Numerical examples of two-element airfoils are treated using this new method of design. The fluid is considered to be incompressible and Reynolds numbers are assumed to be sufficiently large that the boundary layer in the zero skin-friction state is turbulent.

II. DETERMINATION OF OPTIMUM PRESSURE DISTRIBUTION

A. The Zero Skin-Friction Requirement and $C_{L_{max}}$

It is well known that the maximum lift coefficient attainable for a given airfoil is determined by the flow separation which occurs on the upper surface of the airfoil. Generally, the lift coefficient of an airfoil is directly proportional to its angle of attack with respect to the free stream. For angles of attack larger than some particular value, α_1, however, the lift coefficient increases at a slower rate with respect to the increase of angle of attack and even starts to decrease when the angle of attack is increased beyond another particular value, α_2. The reason for this slow increase of lift coefficient and a later decrease is that the boundary layer on the upper surface of the airfoil cannot sustain the steep pressure rise which appears on the upper surface as a result of a large angle of attack. At α_1, a flow separation appears at a point near the trailing edge and generates a small region of reverse flow. This region of reverse flow expands as the angle of attack becomes larger than α_1 and finally develops into a large high pressure region with a large portion of the airfoil upper surface as its boundary.

While flow separation is a local phenomenon, it is apparent that when the flow starts to separate at a certain point on the airfoil surface, the boundary layers at other points may be still able to sustain their local pressure gradient. Therefore, from the viewpoint of generating large lift coefficient, it seems that an airfoil would be more efficient if it could generate a pressure distribution such that the boundary layer separation would occur wherever the pressure is increasing if separation does occur at

all. In other words, an airfoil which can provide a large maximum lift coefficient is the one which has no flow separation for angles of attack smaller than a value α_s, and suddenly stalls at $\alpha = \alpha_s$. This point may be made clear by considering the pressure distribution shown in Figure 1. The lift coefficient of the airfoil which generates this pressure distribution is represented by the area enclosed by the curve $C_p(x)$ where the x-axis is parallel to the free stream. If the flow separates at A, but at no other point, then the skin friction has positive value for every point upstream of A. Now, let the pressure distribution between B and A follow a different curve such as the dotted line in Figure 1. Then, the pressure gradient at points upstream of A will be steeper and the area enclosed by the $C_p(x)$ curve is increased which means that the lift coefficient has been increased too. It is possible that the flow will separate somewhere between A and B with this new pressure distribution. Let it be assumed that the skin friction resulted from pressure distribution (2) is zero everywhere between C and A. It is not hard to see that any attempts to increase the lift coefficient of the airfoil by forcing the pressure distribution to follow a curve such as the one represented by the broken line will steepen the pressure gradient and hence introduce flow separation. The lift coefficient, then, will be decreased. Therefore, among all the pressure distributions which are identical at every point except the region where pressure is increasing, the one which yields zero skin friction over the pressure recovery region provides the maximum lift coefficient. This is the foundation based upon which high lift airfoils of the Liebeck-Ormsbee type are designed. When an additional element is present near the airfoil, such as a trailing edge flap, the argument

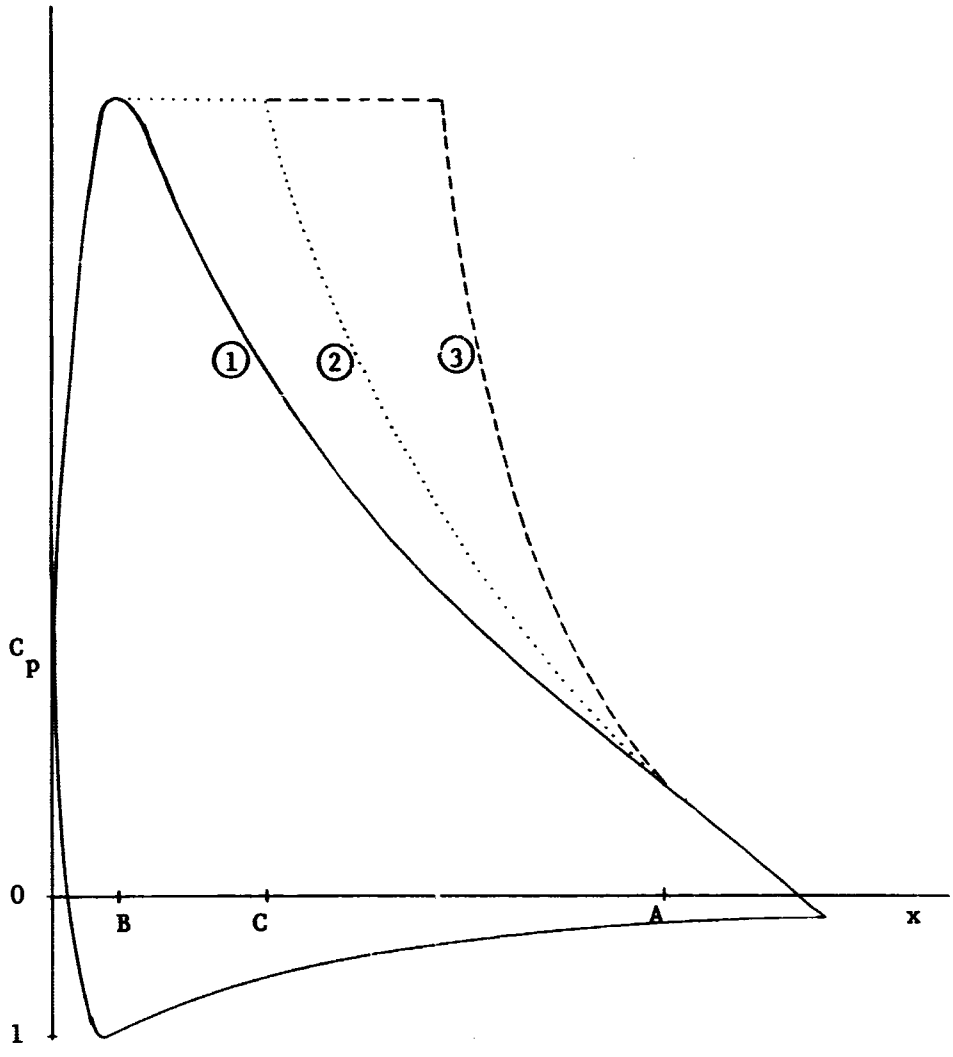

Figure 1. Zero skin friction and $C_{L_{max}}$.

stated above still applies. Namely, the pressure recovery on both the main airfoil and the auxiliary element should yield zero skin friction in order to achieve maximum lift coefficient of the airfoil. In general, a multiple-element airfoil will have maximum lift coefficient if this pressure recovery of zero skin-friction type appears on each element of the airfoil.

B. Variational Problem and Its Solution

1. Stratford's Pressure Distribution and Formulation of the Variational Problem

As stated in Chapter I, the fluid flows are considered to be incompressible. In order to obtain a boundary layer which is capable of sustaining a large positive pressure gradient, only flows with large Reynolds numbers are considered. Based on these two essential assumptions, a problem in the calculus of variations will be formulated in this subsection.

Suppose that the fluid is inviscid. The lift force of an airfoil is given by the Kutta-Joukowski Theorem

$$L = \rho U_\infty \Gamma$$

where ρ is the density of the fluid, U_∞ is the speed at which the airfoil travels in the fluid and Γ is the circulation required to place the rear stagnation point at the trailing edge of the airfoil. With a given airfoil of specified chord length and a specified velocity, the only way to obtain more lift force is to increase the circulation Γ. The circulation Γ, by definition, can be written as

$$\Gamma = \int_0^{s_T} v(s)ds \qquad (1)$$

where s is the arc length of the airfoil contour, measured clockwise from the trailing edge along the airfoil surface (see Figure 2), s_T is the total length of the contour of the airfoil and v(s) is the surface velocity distribution. With subscript L denoting the front stagnation point of the airfoil, the integral (1) can be decomposed into two terms

$$\int_0^{s_L} v(s)ds + \int_{s_L}^{s_T} v(s)ds \qquad (2)$$

where $0 \leq s \leq s_L$ holds for the lower surface and $s_L \leq s \leq s_T$ holds for the upper surface of the airfoil. Notice that along the lower surface, the direction of v is opposite that of increasing s. Therefore, the first term in (2) is a negative one. There is no way that a positive quantity may be obtained as the first term of (2) unless the front stagnation point is forced to coincide with the trailing edge. However, this is physically unattainable. Thus, the most which can be obtained from the lower surface is a zero velocity all the way from the front stagnation point to the trailing edge. In other words, $v(s) = 0$ for $0 \leq s \leq s_L$. With this velocity on the lower surface of an airfoil, variations in lift may occur only by changing the velocity distribution on the upper surface. The circulation then stands as

$$\Gamma = \int_{s_L}^{s_T} v(s)ds \ .$$

For convenience, the origin of s may be shifted from the trailing edge to the front stagnation point. With this modification, the circulation is

$$\int_0^{s_U} v(s)ds$$

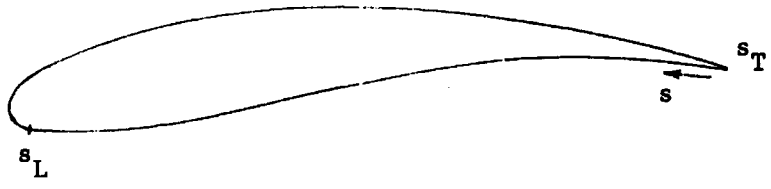

Figure 2. Definition of the variable s.

where $s_U = s_T - s_L$ and subscript U stands for the upper surface. The lift coefficient of the airfoil, based on free stream dynamic head and length s_U of the upper surface, is

$$C_L = \frac{\rho U_\infty}{\frac{1}{2}\rho U_\infty^2 s_U} \int_0^{s_U} v(s)ds$$

or

$$C_L = \frac{2}{s_U} \int_0^{s_U} q(s)ds \qquad (3)$$

where q(s) is the surface velocity normalized with respect to the free stream velocity. This velocity q(s) always starts from the front stagnation point s = 0 with a value of zero, increases monotonically to a maximum value q_0 at a point $s = s_0$ and then decreases monotonically to the value of zero at the trailing edge where $s = s_U$. For the purpose of generating maximum lift coefficient in the way described in Section A above, the function q(s) can be any form for $0 \leq s \leq s_0$. There is no restriction for that part of q(s) other than the one that it must be monotonically non-decreasing. The function q(s) for $s_0 \leq s \leq s_U$, however, must satisfy the requirement of being able to provide a boundary layer of zero skin friction everywhere between s_0 and s_U, with the reason described in Section A. Such a function q(s) may be obtained by modifying the expression derived by Stratford.[2] Stratford considered the turbulent boundary layer grown on a flat plate and derived an expression for predicting the separation of this turbulent boundary layer when an adverse pressure gradient is encountered. Let the leading edge of the flat plate be at the origin x = 0 and let the pressure start to rise at $x = x_0$. Separation will occur when the following equation is satisfied by $C_{P_0}(x)$

$$(2C_{p_0})^{\frac{1}{4}(n-2)} \left(x \frac{dC_{p_0}}{dx}\right)^{\frac{1}{2}} = 1.06\beta (10^{-6}\ \mathrm{Re})^{\frac{1}{10}} \qquad (4)$$

where $C_{p_0}(x)$ is the pressure coefficient based on free stream p_0, U_0; β is a constant which is approximately 0.66 for Reynolds number of order 10^6; n is the common logarithm of Re which is the Reynolds number based on U_0 and x. The criterion employed in deriving (4) is that separation is imminent wherever local skin friction equals zero. Therefore, by treating (4) as a differential equation for $C_{p_0}(x)$, a pressure distribution which provides zero skin friction at every point downstream of x_0 is found to be

$$C_{p_0}\left(\frac{x}{x_0}\right) = 0.645\left\{0.435\ \mathrm{Re}_0^{\frac{1}{5}}\left[\left(\frac{x}{x_0}\right)^{\frac{1}{5}} - 1\right]\right\}^{2/n} \text{ for } C_{p_0} \leq \frac{n-2}{n+1}$$

$$= 1 - \frac{a}{(x+b)^{1/2}} \qquad \text{for } C_{p_0} \geq \frac{n-2}{n+1} \qquad (5)$$

where Re_0 is the Reynolds number based on x_0 and uniform velocity U_0 and n is the common logarithm of Re_0; a and b are constants to be determined such that C_{p_0} and dC_{p_0}/dx are continuous at $C_{p_0} = \frac{n-2}{n+1}$. These derived results have been verified by Stratford[3] and experiments showed that this $C_{p_0}(x/x_0)$ does provide a boundary layer of zero turbulent skin friction.

The pressure starts to rise at $s = s_0$ on an airfoil where $q = q_0$. Hence the relation between q(s) and $C_{p_0}(x/x_0)$ is established by first setting $U_0 = q_0 U_\infty$. Then, since

$$q = \frac{U}{U_\infty} = \frac{U}{U_0}\frac{U_0}{U_\infty} \quad \text{and} \quad C_{p_0} = 1 - \left(\frac{U}{U_0}\right)^2$$

one obtains

$$q(s) = q_0\left[1 - C_{p_0}\left(\frac{x}{x_0}\right)\right]^{1/2} . \qquad (6)$$

It should be pointed out, however, that expression (5) above was derived when the boundary layer on a flat plate in a uniform flow was under consideration. For a non-decreasing velocity distribution U(s) the relation between s_0 and x_0 is

$$x_0 = \int_0^{s_0} \left[\frac{U(s)}{U_0}\right]^3 ds \qquad (7)$$

which merely states that the momentum thickness of the boundary layer at $s = s_0$ on an airfoil with velocity distribution U(s) for $0 \leq s \leq s_0$ has been set to be the same as that of the boundary layer at $x = x_0$ on a flat plate in a uniform flow. Now, with the small velocity near the front stagnation point, the boundary layer there is likely to be laminar. This laminar initial boundary layer is acceptable provided a transition to turbulent boundary layer has taken place before the pressure starts to increase. This is because Stratford considered only the separation of turbulent boundary layers. With this laminar boundary layer present, equation (7) is superseded by

$$x_0 = 38.2\left(\frac{\nu}{s_t U_t}\right)^{3/8} \left(\frac{U_0}{U_t}\right)^{1/8} \left[\int_0^{s_t} \left(\frac{U}{U_0}\right)^5 d\left(\frac{s}{s_t}\right)\right]^{5/8} s_t + \int_{s_t}^{s_0} \left(\frac{U}{U_0}\right)^3 ds \qquad (8)$$

where subscript t indicates that the variables are evaluated at the transition point. An instantaneous transition with the preservation of

momentum thickness has been assumed in deriving equation (8). Therefore, a boundary layer which is entirely laminar between $s = 0$ and $s = s_0$ is acceptable provided an instantaneous transition takes place at s_0. In order to have pressure increase at s_0, the starting point of $q(s)$ will not be the same as the equivalent flat plate boundary layer. This is illustrated in Figure 3. Hence equation (6) must be used with the understanding that s and x are related by equation (8) and Figure 3.

Now, with an arbitrary acceleration $q(s)$ for $0 \leq s \leq s_0$ and a pressure rise of the Stratford's type described by (5), the lift coefficient of the airfoil is

$$C_L = \frac{2}{s_U}\left\{\int_0^{s_0} q(s)ds + \int_{s_0}^{s_U} q_0\left[1 - C_{p_0}\left(\frac{x}{x_0}\right)\right]^{1/2}ds\right\}$$

where C_{p_0} is given by equation (5) with x_0 defined in equation (8) and the relation between x and s is shown in Figure 3. In this expression, s_U can be considered a constant. s_0 is not specified. $q(s)$ is any monotonically increasing function. q_0 is not specified and the function C_{p_0} depends on x/x_0 and Re_0 only. These quantities can be varied in order that a maximum value of C_L may be obtained. Among these quantities, Re_0 should be specified independent of the others because Re_0 specifies the boundary layer characteristics at s_0 and hence the zero skin friction pressure recovery $C_{p_0}(x/x_0)$. When Re_0 and s_U are given, the problem of finding the maximum value of C_L becomes one of searching for a function $q(s)$ and values of the quantities s_0, q_0 such that the quantity

$$C_L = \frac{2}{s_U}\left\{\int_0^{s_0} q(s)ds + \int_{s_0}^{s_U} q_0\left[1 - C_{p_0}\left(\frac{x}{x_0}\right)\right]^{1/2}ds\right\}$$

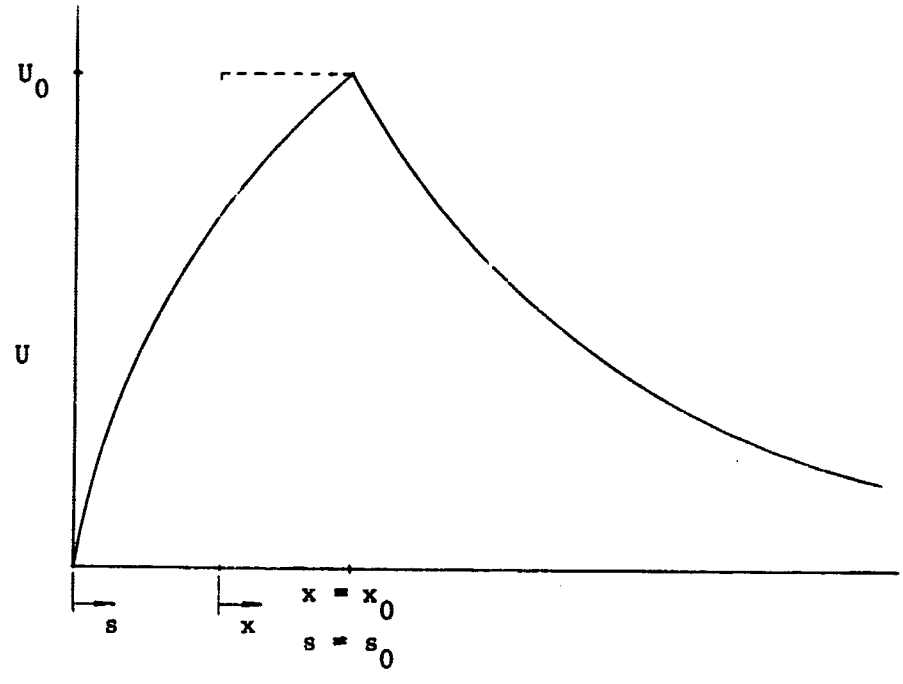

Figure 3. Relation between s and Stratford's x.

takes its maximum value. x_0 is to be computed from equation (8). This is a problem of calculus of variations for the funtion q(s). For q_0 and s_0, it is a problem of differential calculus.

As can be easily seen from the results obtained by Stratford, the pressure recovery with zero skin friction has a large pressure gradient immediately downstream of x_0. When the value of x is very large, the rate of increase of pressure is very slow. In the limit, C_{p_0} will reach a value of one only if x goes to infinity. This means that the zero skin friction pressure recovery, when produced by an airfoil, will reach stagnation at the trailing edge only if the airfoil has an infinite chord length. In view of the fact that an airfoil with a chord of infinite length is not practical, a non-zero value of q_U will be accepted as the trailing edge velocity. This leads to a sharp trailing edge which is acceptable for aerodynamic consideration. Now, the three quantities s_0, q_0 and q_U are related to each other once an Re_o and an s_U are given. Only the value of one of them may be specified and the solution to the variational problem will determine the others. Suppose the value of s_0 is specified. Then q_U can always be obtained for a given q_0. The consequence is that there are infinitely many sets of q_0 and q_U which can yield zero skin friction pressure recovery. The maximum lift coefficient which may be obtained under this circumstance has no upper bound. This indicates that the problem is not well defined. Alternatively, if q_0 is specified, the lift coefficient will take a maximum value only when s_0 goes to zero, and this solution does not make any physical sense. Therefore, the only remaining possibility is to specify the value of q_U and let the values of q_0 and s_0 be determined by the solution of the variational problem. Therefore, the problem can be

redefined as one of finding a function $q(s)$ for $0 \leq s \leq s_0$ and two quantities q_0 and s_0 in order that

$$C_L = \frac{2}{s_U} \left\{ \int_0^{s_0} q(s)ds + \int_{s_0}^{s_U} q_0 \left[1 - C_{p_0} \left(\frac{x}{x_0}\right)\right]^{1/2} ds \right\} \tag{9}$$

has a maximum value. The values of Re_0, s_U and q_U are specified and x_0 is to be computed from equation (8). Since equation (8) takes a simpler form if the boundary layer is turbulent from $s = 0$ to $s = s_0$, the case of having a laminar initial boundary layer will be considered after the simpler case of an all turbulent boundary layer is treated.

2. Solution to the Variational Problem When Boundary Layer Is All Turbulent

When the boundary layer is all turbulent, equation (8) becomes

$$x_0 = \int_0^{s_0} \left[\frac{q(s)}{q_0}\right]^3 ds \ . \tag{10}$$

For the convenience of algebraic manipulation, it is desirable to make a transformation on the variable s. With the definition of a constant $\kappa = s_0/x_0$, the relation between s and x is

$$s = x + (k - 1)\, x_0$$

or

$$x = s - (k - 1)\, x_0 \ .$$

Dividing x by x_0, a variable z may be defined as

$$z = \frac{x}{x_0}$$

$$= \frac{s}{x_0} - (k - 1) \ .$$

With this notation, equation (9) may be written as

$$C_L = \frac{2}{Z+k-1} \left\{ \int_{-(k-1)}^{1} q(z)dz + q_0 \int_{1}^{Z} [1 - C_{p_0}(z)]^{1/2} \, dz \right\} \qquad (11)$$

where Z denotes the value of z at the trailing edge. Now, the function C_{p_0} may take only one form of equation (5) or both depending on the values of Re_0 and x/x_0. For Re_0 of order 10^6 - 10^8, C_{p_0} will reach the value $\frac{n-2}{n+1}$ for a fairly small value of x/x_0. Hence it can be assumed that C_{p_0} will take the value $\frac{n-2}{n+1}$ at a point s_m which is between s_0 and s_U for the Reynolds numbers considered in this research. With this assumption, Stratford's equation (29),[2] which expresses the function $C_{p_0}(x/x_0)$ for $C_{p_0} \geq \frac{n-2}{n+1}$, can be modified to give

$$q_0 = q_U \frac{(Z+b')^{1/4}}{\sqrt{a'}} \qquad (12)$$

where $a' = a/x_0$, $b' = b/x_0$. Hence equation (11) becomes

$$C_L = \frac{2}{Z+k-1} \int_{1-k}^{1} q(z)dz + \frac{2}{Z+k-1} \frac{q_U(Z+b')^{1/4}}{\sqrt{a'}}$$

$$\times \int_{1}^{Z_m} \{1-0.645[0.435\ Re_0^{1/5}(z^{1/5}-1)]^{2/n}\}^{1/2} \, dz$$

$$+ \frac{2}{Z+k-1} \, q_U(Z+b')^{1/4} \int_{Z_m}^{Z} \frac{dz}{(z+b')^{1/4}} \qquad (13)$$

where $Z_m = s_m/x_0 - (k - 1)$, and equation (10) becomes

$$1 = \int_{1-k}^{1} \left[\frac{q(z)}{q_0}\right]^3 dz \ . \qquad (14)$$

To find a stationary value of C_L, the variation of C_L caused by the variation of the right hand side of equation (13) must vanish. This variation includes the variation of q(z), the variation of k and the variation of Z. The variation of k is related to that of q(z) by the constraint equation (14). Hence only the variation of q(z) and Z need to be considered. The appearance of q(z) inside an integral sign makes the problem fall into the category of calculus of variations. However, due to the simplicity of the integrands which contain q(z) in both equation (13) and equation (14), the solution to this problem of calculus of variations can be obtained in a quite simple way. Because no derivatives of q(z) appear in the integrand, the Euler's equation resulted from the vanishing of first variation of C_L is an algebraic equation instead of a differential equation. The solution to that equation is merely q(z) = constant. This constant, then, is determined by the requirement that $q(s_0) = q_0$. Substitution of $q(z) = q_0$ into equation (14) gives k = 1. Therefore, as far as q(z) is concerned, C_L will have a stationary value only when $q(z) = q_0$. The fact that the value of C_L provided by this q(z) is really a maximum one may be established in the following way. Suppose a permissible variation is introduced into this function q(z). Permissible means that q(z) is still a monotonically non-decreasing function. The value of k will always increase. The value of $\int_{1-k}^{1} q(z)dz$ may increase or it may decrease. Because of the constraint of equation (14), the increase of k is so large that C_L will always be decreased by this variation of q(z). Therefore, in order to obtain a maximum lift coefficient, the fluid should be accelerated abruptly from the front stagnation point to a velocity q_0 and remain at that value until pressure starts to increase.

With this conclusion, equation (13) becomes

$$C_L = \frac{2}{Z}\frac{q_U(Z+b')^{1/4}}{\sqrt{a'}} + \frac{2}{Z}\frac{q_U(Z+b')^{1/4}}{\sqrt{a'}} \times \int_1^{Z_m} \{1-0.645[0.435\ Re_0^{1/5}(z^{1/5}-1)]^{2/n}\}^{1/2}\, dz + \frac{2}{Z}\frac{q_U(Z+b')^{1/4}}{\sqrt{a'}} \int_{Z_m}^{Z} \frac{\sqrt{a'}}{(z+b')^{1/4}}\, dz \ .$$

Since Z_m depends on Re_0 only, the integral in the second term may be abbreviated as

$$I(Re_0) \equiv \int_1^{Z_m} \{1-0.645[0.435\ Re_0^{1/5}(z^{1/5}-1)]^{2/n}\}^{1/2}\, dz \ .$$

This allows C_L to be expressed as

$$C_L = \frac{2q_U(Z+b')^{1/4}}{Z\sqrt{a'}} \{1 + I(Re_0) + \frac{4}{3}\sqrt{a'}[(Z+b')^{3/4} - (Z_m+b')^{3/4}]\}$$

where the integration appearing in the last term has been carried out. With values of q_U and Re_0 given, this C_L varies with Z only. The maximum value of C_L may be obtained by evaluating C_L at a value of Z where the first derivative of C_L with respect to Z vanishes. Taking the first derivative of C_L with respect to Z and setting the result equal to zero gives

$$\frac{3}{4}[1 + I(Re_0) - \frac{4}{3}\sqrt{a'}(Z_m+b')^{3/4}](Z+b') + \frac{4}{3}\sqrt{a'b'}\ (Z+b')^{3/4} + \frac{b'}{4}[1 + I(Re_0) - \frac{4}{3}\sqrt{a'}(Z_m+b')^{3/4}] = 0 \ . \qquad (15)$$

This is a fourth degree algebraic equation for $(Z+b')^{1/4}$ and there are four roots. The second derivative d^2C_L/dZ^2 must be evaluated at each root of equation (15) in order to find out which root gives the maximum value of C_L. The expression for d^2C_L/dZ^2 is

$$\frac{2q_U}{\sqrt{a'}}\{[1 + I(Re_0) - \frac{4}{3}\sqrt{a'}(Z_m+b')^{3/4}][\frac{2(Z+b')^{1/4}}{Z^3} - \frac{(Z+b')^{-3/4}}{2Z^2} - \frac{3(Z+b')^{-7/4}}{16Z}] + \frac{8}{3}\sqrt{a'b'}\ \frac{1}{Z^3}\} . \qquad (16)$$

For $5 \times 10^5 \leq Re_0 \leq 1 \times 10^8$, equation (15) has two conjugate complex roots, one negative real root and one positive real root. In view of equation (12) only positive values of $(Z+b')^{1/4}$ can be accepted. Computations have shown that this positive root of equation (15) gives a value Z which is larger than Z_m and this Z does yield a negative value of d^2C_L/dZ^2. Substituting this Z into equation (12) gives the value of q_0/q_U and thus the solution to the variational problem is complete for an all turbulent boundary layer. (See Figure 4). The dependence of Z_m, Z, and q_0/q_U on Re_0 is given in Table 1. Also shown in Table 1 are the values of d^2C_L/dZ^2.

3. Solution to the Variational Problem When the Initial Boundary Layer Is Laminar

When a laminar initial boundary layer is present, the full expression (8) must be used as the constraint on q(s) for $0 \leq s \leq s_0$. Using the definition of q, equation (8) can be rewritten as

$$x_0 = 38.2\ (\frac{\nu}{s_t U_t})^{3/8}(\frac{q_0}{q_t})^{1/8}\{\int_0^{s_t}[\frac{q(s)}{q_0}]^5\ d(\frac{s}{s_t})\}^{5/8}\ s_t + \int_{s_t}^{s_0}[\frac{q(s)}{q_0}]^3\ ds . \qquad (17)$$

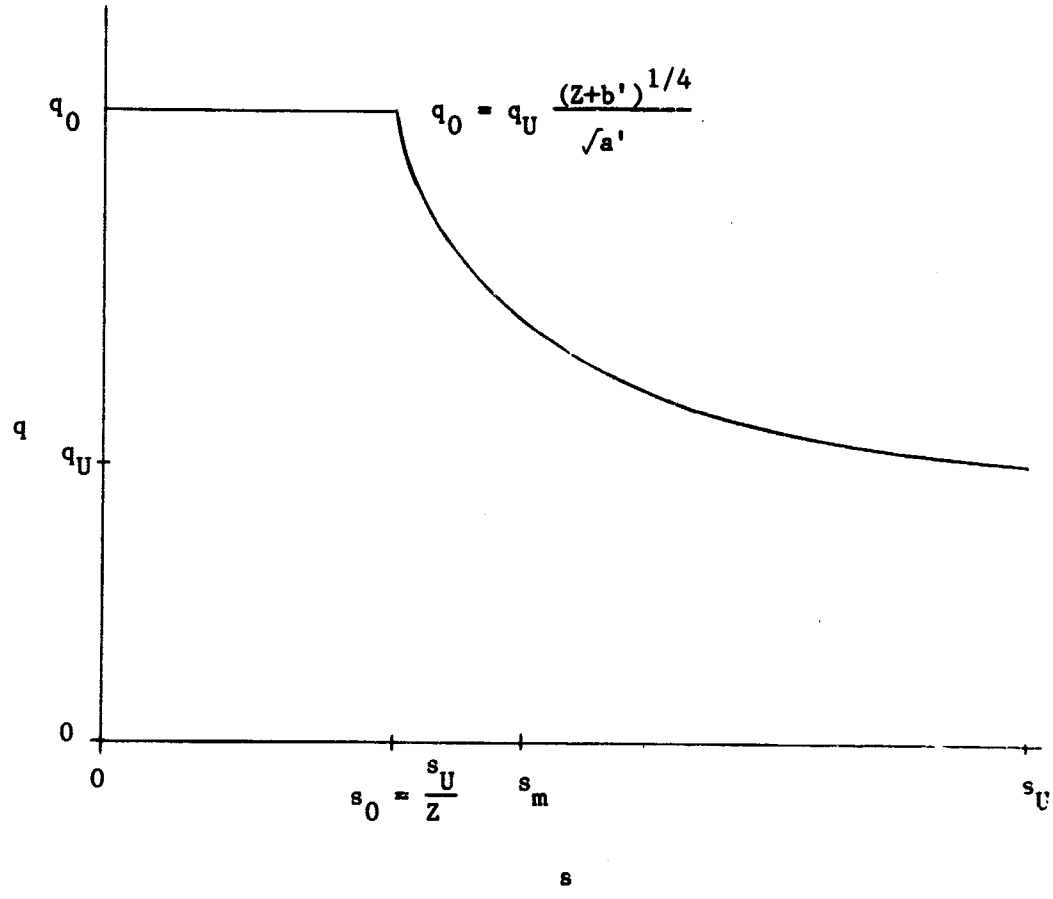

Figure 4. Optimized velocity distribution on the upper surface of a single-element airfoil with all turbulent boundary layer.

Table 1

Dependence of Z_m, Z, q_0/q_U and d^2C_L/dZ^2 on Re_0 for an All Turbulent Boundary Layer

$Re_0 \times 10^{-5}$	Z_m	Z	q_0/q_U	d^2C_L/dZ^2
5	1.6625	4.2340	2.0822	-0.003332
6	1.6502	4.0713	2.0824	-0.003887
7	1.6400	3.9473	2.0835	-0.004395
8	1.6313	3.8487	2.0852	-0.004863
9	1.6236	3.7677	2.0872	-0.005298
10	1.6168	3.6995	2.0893	-0.005705
20	1.5735	3.3312	2.1099	-0.008790
30	1.5493	3.1640	2.1264	-0.010926
40	1.5327	3.0611	2.1397	-0.012587
50	1.5201	2.9887	2.1508	-0.013959
60	1.5101	2.9338	2.1603	-0.015134
70	1.5017	2.8900	2.1686	-0.016164
80	1.4945	2.8538	2.1761	-0.017085
90	1.4883	2.8233	2.1828	-0.017917
100	1.4827	2.7969	2.1889	-0.018678
200	1.4478	2.6430	2.2318	-0.023071
300	1.4285	2.5662	2.2587	-0.027529
400	1.4154	2.5165	2.2784	-0.030114
500	1.4054	2.4804	2.2942	-0.032193
600	1.3974	2.4523	2.3073	-0.033938
700	1.3908	2.4295	2.3185	-0.035447
800	1.3852	2.4104	2.3283	-0.036779
900	1.3802	2.3940	2.3371	-0.037970
1000	1.3759	2.3797	2.3450	-0.039051

Now, by defining $g = s_t/s_0$ and replacing s by z, equation (17) becomes

$$1 = 38.2\left(\frac{\nu}{x_0 U_\infty q_t}\right)^{3/8}\left(\frac{q_0}{q_t}\right)^{1/8}\left\{\int_{1-k}^{1-k+gk}\left[\frac{q(z)}{q_0}\right]^5 dz\right\}^{5/8} + \int_{1-k+gk}^{1}\left[\frac{q(z)}{q_0}\right]^3 dz \quad (18)$$

Since the expression for C_L, equation (9), holds true whether the initial boundary layer is laminar or turbulent, the problem is again to find a q(z) which will give a maximum value of

$$C_L = \frac{2}{Z+k-1}\int_{1-k}^{1} q(z)dz + \frac{2}{Z+k-1}\frac{q_U(Z+b')^{1/4}}{\sqrt{a'}} \times \int_{1}^{Z_m}\left\{1-0.645\left[0.435\ Re_0^{1/5}(z^{1/5}-1)\right]^{2/n}\right\}^{1/2} dz + \frac{2}{Z+k-1}\,q_U(Z+b')^{1/4}\int_{Z_m}^{Z}\frac{dz}{(z+b')^{1/4}} \quad (13)$$

It can be seen that no derivatives of the function q(z) appear in the integral terms in equation (13) and equation (18). Thus, the solution to this variational problem is again $q(z) = q_0$ for $0 \le s \le s_0$. With this q(z), equation (18) gives

$$1 = 38.2\left(\frac{\nu}{x_0 U_0}\right)^{3/8}(gk)^{5/8} + (1-g)k \ . \quad (19)$$

The critical Reynolds number at which boundary layer transition takes place is defined by

$$Re_{cr} = \frac{s_t U_0}{\nu}$$

which is

$$Re_{cr} = \frac{gs_0U_0}{\nu}$$

$$= \frac{gkx_0U_0}{\nu} \quad .$$

Hence,

$$gk = \frac{Re_{cr}}{Re_0} \quad .$$

Substituting this gk into equation (19) gives

$$k = 1 - 38.2\, Re_0^{-1}\, Re_{cr}^{5/8} + \frac{Re_{cr}}{Re_0} \quad . \qquad (20)$$

This result requires that a critical Reynolds number Re_{cr} be specified in addition to the Reynolds number Re_0 when the initial boundary layer is laminar. Notice that the case $Re_{cr} > Re_0$ need not be excluded because an all-laminar boundary layer between $s = 0$ and s_0 will give $k > 1$ and $g = 1$. When the boundary layer is all turbulent $g = 0$ and equation (19) gives $k = 1$ which is the result obtained in the previous subsection. With $q(z) = q_0$ and k given by (20), equation (13) can be written as

$$C_L = \frac{2}{k+Z-1} \frac{(Z+b')^{1/4}}{\sqrt{a'}} q_U\{k + I(Re_0) + \frac{4}{3}\sqrt{a'}$$

$$\times [(Z+b')^{3/4} - (Z_m+b')^{3/4}]\} \qquad (21)$$

where Z, $I(Re_0)$ and Z_m all have the same meaning as in the previous subsection. When the laminar initial boundary layer is absent, $g = 0$ gives $k = 1$ which reduces equation (21) to the form assumed by an all turbulent boundary layer given in Subsection 2. This verifies the consistency of the expressions derived up to this stage.

To find the maximum value of C_L with various Z values, the derivative dC_L/dz is set to zero and the second derivative d^2C_L/dZ^2 must be evaluated at certain Z values. The equation which results from setting dC_L/dZ to zero is

$$\frac{3}{4}\left[k + I(Re_0) - \frac{4}{3}\sqrt{a'}(Z_m+b')^{3/4}\right](Z+b') - \frac{4}{3}\sqrt{a'}(k-1-b')(Z+b')^{3/4}$$

$$- \frac{1}{4}(k-1-b')\left[k+I(Re_0) - \frac{4}{3}\sqrt{a'}(Z_m+b')^{3/4}\right] = 0 . \qquad (22)$$

As in the equation obtained in Subsection 2, this is also a fourth degree algebraic equation for the variable $(Z+b')^{1/4}$. For $2 \times 10^5 \leq Re_0 \leq 1 \times 10^7$, two different values have been used for Re_{cr}. They are 5×10^5 and 1×10^6. In both cases, there are always two conjugate complex roots, one negative real root and one positive real root. As stated in the previous subsection, only the positive real root is retained, and it does give a negative value of d^2C_L/dZ^2 when this positive real root is substituted into

$$\frac{2q_U}{\sqrt{a'}}\left\{\left[k + I(Re_0) - \frac{4}{3}\sqrt{a'}(Z_m+b')^{3/4}\right]\left[-\frac{3}{16}\frac{(Z+b')^{-7/4}}{k+Z-1}\right.\right.$$

$$\left. - \frac{(Z+b')^{-3/4}}{2(k+Z-1)^2} + \frac{2(Z+b')^{1/4}}{(k+Z-1)^3}\right]$$

$$\left. - \frac{8}{3}\frac{\sqrt{a'}}{(k+Z-1)^2} + \frac{8}{3}\frac{\sqrt{a'}(Z+b')}{(k+Z-1)^3}\right\} .$$

This means that a maximum value of C_L does exist at this Z. Substituting this Z into equation (12) gives the value of q_0/q_U. The dependence of g, Z_m, Z and q_0/q_U on Re_0 are shown in Table 2 and Table 3. Also shown

Table 2

Dependence of g, k, Z_m, Z, q_0/q_U and d^2C_L/dZ^2 on Re_0 for Boundary Layers Which are Initially Laminar, $Re_{cr} = 5 \times 10^5$

$Re_0 \times 10^{-4}$	g	k	Z_m	Z	q_0/q_U	d^2C_L/dZ^2
15	0.979	3.404	1.7462	6.7252	2.1895	-0.002548
20	0.892	2.804	1.7258	6.0092	2.1656	-0.003025
25	0.819	2.443	1.7101	5.5548	2.1512	-0.003417
30	0.757	2.202	1.6974	5.2363	2.1419	-0.003754
35	0.704	2.031	1.6868	4.9983	2.1355	-0.004053
40	0.657	1.902	1.6776	4.8121	2.1331	-0.004323
45	0.617	1.802	1.6696	4.6613	2.1280	-0.004573
50	0.581	1.721	1.6625	4.5361	2.1257	-0.004806
55	0.549	1.656	1.6561	4.4299	2.1241	-0.005026
60	0.520	1.601	1.6502	4.3384	2.1230	-0.005235
65	0.495	1.555	1.6449	4.2584	2.1222	-0.005435
70	0.471	1.515	1.6400	4.1876	2.1217	-0.005627
75	0.450	1.481	1.6355	4.1245	2.1214	-0.005811
80	0.431	1.451	1.6313	4.0677	2.1213	-0.005990
85	0.413	1.424	1.6273	4.0161	2.1213	-0.006163
90	0.397	1.401	1.6236	3.9691	2.1215	-0.006331
95	0.381	1.380	1.6201	3.9260	2.1217	-0.006494
100	0.367	1.361	1.6168	3.8863	2.1219	-0.006653
200	0.212	1.180	1.5735	3.4410	2.1236	-0.009236
300	0.149	1.120	1.5493	3.2423	2.1441	-0.011152
400	0.115	1.090	1.5327	3.1219	2.1543	-0.012697
500	0.093	1.072	1.5201	3.0385	2.1633	-0.013998
600	0.079	1.060	1.5101	2.9759	2.1712	-0.015127
700	0.068	1.052	1.5017	2.9264	2.1784	-0.016127
800	0.060	1.045	1.4945	2.8860	2.1849	-0.017026
900	0.053	1.040	1.4883	2.8520	2.1909	-0.017842
1000	0.048	1.036	1.4827	2.8229	2.1964	-0.018592

Table 3

Dependence of g, k, Z_m, Z, q_0/q_U and d^2C_L/dZ^2 on Re_0 for Boundary Layers Which are Initially Laminar, $Re_{cr} = 10^6$

$Re_0 \times 10^{-4}$	g	k	Z_m	Z	q_0/q_U	d^2C_L/dZ^2
25	0.966	4.141	1.7101	6.8501	2.2816	-0.002902
30	0.922	3.617	1.6974	6.3104	2.2585	-0.003317
35	0.881	3.243	1.6868	5.9131	2.2412	-0.003689
40	0.843	2.963	1.6776	5.6070	2.2277	-0.004026
45	0.810	2.745	1.6696	5.3630	2.2171	-0.004336
50	0.778	2.570	1.6625	5.1634	2.2085	-0.004621
55	0.749	2.428	1.6561	4.9965	2.2014	-0.004886
60	0.722	2.309	1.6502	4.8547	2.1955	-0.005133
65	0.697	2.208	1.6449	4.7323	2.1906	-0.005366
70	0.673	2.122	1.6400	4.6255	2.1865	-0.005587
75	0.651	2.047	1.6355	4.5313	2.1829	-0.005796
80	0.631	1.981	1.6313	4.4475	2.1799	-0.005995
85	0.612	1.924	1.6273	4.3723	2.1773	-0.006185
90	0.593	1.872	1.6236	4.3044	2.1751	-0.006368
95	0.577	1.827	1.6201	4.2427	2.1732	-0.006544
100	0.560	1.785	1.6168	4.1864	2.1715	-0.006713
200	0.359	1.393	1.5735	3.5887	2.1621	-0.009317
300	0.264	1.262	1.5493	3.3415	2.1660	-0.011179
400	0.209	1.196	1.5327	3.1970	2.1719	-0.012677
500	0.173	1.157	1.5201	3.0990	2.1782	-0.013944
600	0.147	1.131	1.5101	3.0266	2.1842	-0.015049
700	0.128	1.112	1.5017	2.9702	2.1900	-0.016030
800	0.114	1.098	1.4945	2.9244	2.1953	-0.016916
900	0.102	1.087	1.4883	2.8863	2.2004	-0.017722
1000	0.092	1.079	1.4827	2.8538	2.2051	-0.018465

are the values of d^2C_L/dZ^2. The velocity distribution $q(s)$ for $0 \leq s \leq s_U$ is sketched in Figure 5. Notice that the location where pressure starts to increase is different from the one shown in Figure 4 This is due to the presence of the laminar initial boundary layer

C. The Pressure Distribution To Be Used in Designing Two-Element Optimum Airfoils

The optimum pressure distribution which will provide an airfoil with maximum lift coefficient, as shown in Section B, consists of a constant stagnation pressure along the lower surface of the airfoil, and an abrupt pressure drop to a minimum value which covers a certain distance on the upper surface of the airfoil until the pressure starts to increase according to Stratford's zero skin friction pressure distribution. The determination of geometries of multiple-element airfoils is the main object of this research. Pressure distributions will now be considered which are optimum with respect to $C_{L_{max}}$ for this case. The lift force is again $\rho U_\infty \Gamma$ according to the Kutta-Joukowski Theorem where Γ is the total circulation of the airfoil and can be written as

$$\Gamma = \int_0^{s_{L_1}} v_1(s_1)ds_1 + \int_{s_{L_1}}^{s_{T_1}} v_1(s_1)ds_1 + \int_0^{s_{L_2}} v_2(s_2)ds_2 + \int_{s_{L_2}}^{s_{T_2}} v_2(s_2)ds_2$$

for airfoils consisting of two elements. Contour length is again denoted by s which is measured clockwise from the trailing edge of each element; subscript 1 denotes element one and subscript 2 denotes element

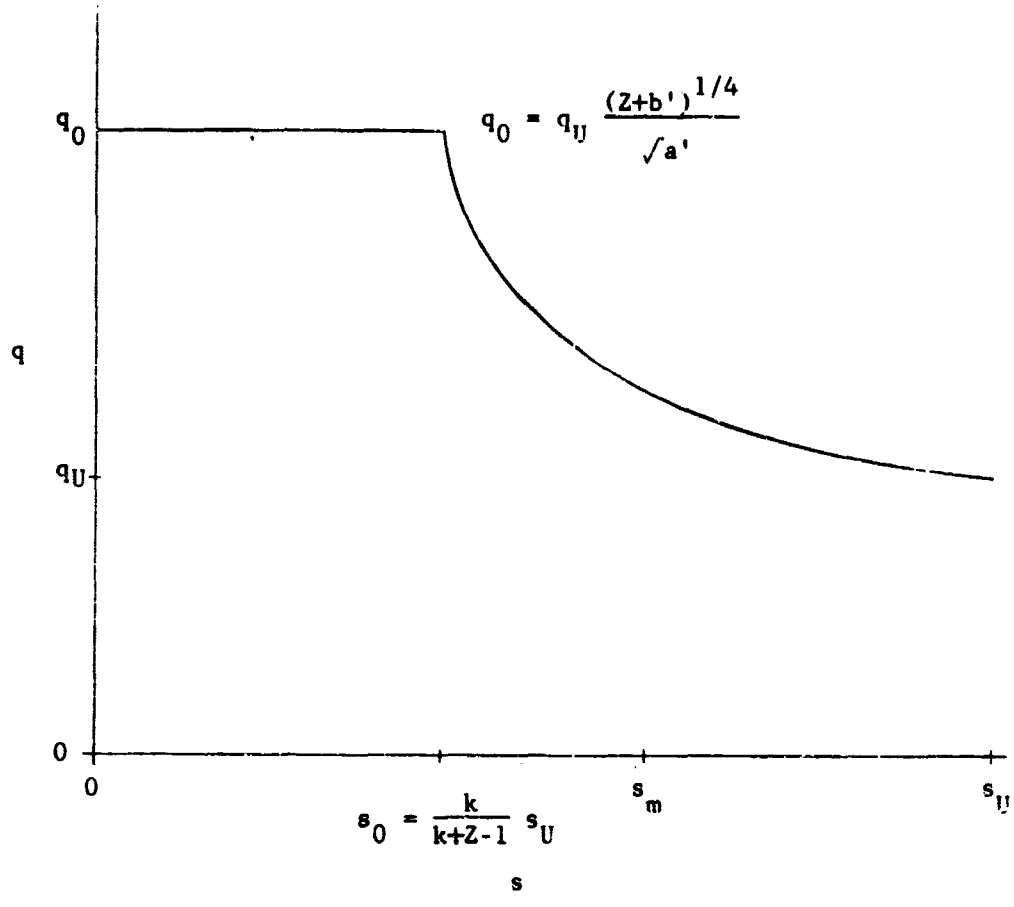

Figure 5 Optimized velocity distribution on the upper surface of a single-element airfoil with laminar initial boundary layer.

two. The first term and the third term are negative quantities since the surface velocity is opposite the direction of increasing s. The maximum value of these quantities is zero. Thus, only two terms are left and the lift coefficient may be written as

$$C_L = \frac{2}{\ell}\int_{s_{L_1}}^{s_{T_1}} q_1(s_1)ds_1 + \frac{2}{\ell}\int_{s_{L_2}}^{s_{T_2}} q_2(s_2)ds_2$$

where ℓ is a characteristic length. For the convenience of manipulation, $s_{T_1} - s_{L_1}$ can be taken as ℓ. This is not only convenient, it is also a more-or-less traditional way because $s_{T_1} - s_{L_1}$ is approximately the chord length of element one. When the origin of measuring s is moved to the front stagnation point of each element as was done in Subsection B.1, C_L becomes

$$C_L = \frac{2}{s_{U_1}}\int_0^{s_{U_1}} q_1(s_1)ds_1 + \frac{s_{U_2}}{s_{U_1}}\,\frac{2}{s_{U_2}}\int_0^{s_{U_2}} q_2(s_2)ds_2 .$$

The first term represents the contribution of element one to C_L, and it has exactly the same form as equation (3). The second term represents the contribution of element two to C_L, and it has the same form as equation (3) except for a multiplicative factor s_{U_2}/s_{U_1}. C_L is to be maximized under the condition that pressure rise on upper surface of each element must yield a boundary layer of zero skin friction in the region where pressure is increasing. This requirement of obtaining maximum lift coefficient has been established in Section A. The pressure rise of zero skin friction is specified by a Reynolds number Re_0. In the case of two-element airfoils, the specification of Re_0 on

one element is entirely independent of that on the other. Furthermore, the pressure distribution on element one can be specified without considering the pressure distribution on element two. In other words, the pressure distributions of two elements are independent. This fact can be easily seen when one realizes that the pressure distribution is specified along the surface contour and the relative position of the two elements is a free parameter at this stage. Therefore, assuming s_{U_2}/s_{U_1} to be a constant, C_L will have a maximum value when both

$$C_{L_1} \equiv \frac{2}{s_{U_1}} \int_0^{s_{U_1}} q_1(s_1)ds_1$$

and

$$C_{L_2} \equiv \frac{2}{s_{U_2}} \int_0^{s_{U_2}} q_2(s_2)ds_2$$

take their maximum values. With Re_0 and q_U given on each element, the problem of maximizing C_L is equivalent to the problem of maximizing the lift coefficients of two single-element airfoils. The solution to this problem has been presented in Subsections B.2 and B.3. This means that for an airfoil consisting of two elements, the maximum lift coefficient will be obtained when the pressure distribution on the surface of each element is such that it is an optimum pressure distribution if each element were considered to be a single-element airfoil with same values of Re_0 and q_U (see Figure 6).

This result can be extended to airfoils consisting of any number of elements. Namely, for a multiple-element airfoil, the maximum lift coefficient will be obtained when the pressure distribution on each

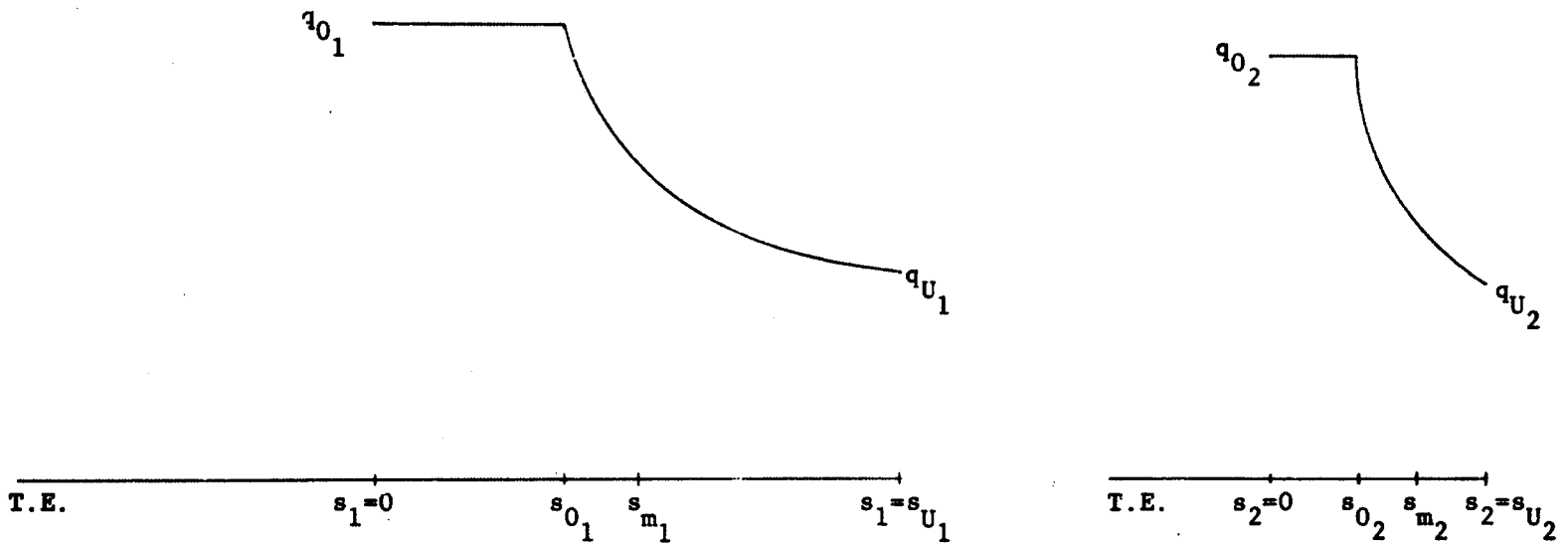

Figure 6. Optimized velocity distribution for a two-element airfoil.

element is composed of a constant stagnation pressure along the lower surface, an abrupt drop to a minimum pressure at the front stagnation point followed by a constant minimum pressure which covers a certain distance on the upper surface until the pressure starts to rise according to Stratford's zero skin friction pressure distribution. It can be recalled that the characteristic length s_U for a single element airfoil will not be available until values of ρ, U_∞, μ, Re_0 are specified. Hence s_U is part of the solution to the variational problem. This confirms the validity of assuming s_{U_2}/s_{U_1} to be a constant when maximizing C_L of a two-element airfoil. Table 4 shows the dependence of s_U on Re_0 for U_∞ = 200 fps., $\mu/\rho = 160 \times 10^{-6}$ ft^2/sec. This makes it possible to design two-element airfoils whose elements have the desirable chord ratios.

Although the pressure distribution shown in Figure 6 provides an airfoil with a maximum lift coefficient, some modifications have to be made in order to realize a physically meaningful airfoil. First, the constant stagnation pressure along the lower surface is not possible to obtain. Since the lower surface of an airfoil does not contribute much to the lift force, any modification of the constant stagnation pressure distribution will not reduce the C_L value too much from its original value. However, a pressure distribution which is monotonically decreasing from leading edge to trailing edge is preferred, and a linear form for q is chosen in this study. A monotonically decreasing pressure from leading edge to trailing edge will produce a boundary layer which always attaches to the airfoil surface, and a linear relation q(s) is chosen for its simplicity. As will be seen in the next chapter, the

Table 4

Dependence of s_U on Re_0 for U_∞ = 200 fps., $\mu/\rho = 160 \times 10^{-6}$ ft^2/sec.

All Turbulent Boundary Layers		Boundary Layers Which are Initially Laminar		
			$Re_{cr} = 5\times10^5$	$Re_{cr} = 10^6$
$Re_0 \times 10^{-5}$	s_U(ft.)	$Re_0 \times 10^{-4}$	s_U(ft.)	s_U(ft.)
5	0.8134	15	0.5004	--
6	0.9385	20	0.5772	--
7	1.0609	25	0.6506	0.8758
8	1.1813	30	0.7215	0.9487
9	1.2997	35	0.7905	1.0190
10	1.4166	40	0.8580	1.0874
20	2.5262	45	0.9242	1.1542
30	3.5711	50	0.9893	1.2196
40	4.5780	55	1.0535	1.2840
50	5.5584	60	1.1168	1.3475
60	6.5186	65	1.1794	1.4101
70	7.4627	70	1.2413	1.4720
80	8.3933	75	1.3025	1.5332
90	9.3126	80	1.3632	1.5939
100	10.2219	85	1.4234	1.6540
200	18.9482	90	1.4831	1.7137
300	27.2677	95	1.5424	1.7728
400	35.3434	100	1.6012	1.8316
500	43.2462	200	2.7169	2.9463
600	51.0170	300	3.7638	3.9926
700	58.6308	400	4.7713	4.9995
800	66.2549	500	5.7517	5.9794
900	73.7533	600	6.7117	6.9388
1000	81.1843	700	7.6554	7.8820
		800	8.5856	8.8116
		900	9.5045	9.7299
		1000	10.4134	10.6383

pressure distribution along the airfoil contour is specified in terms of q, not C_p. Therefore, the modified pressure distribution is a linear q(s) from the front stagnation point where q = 0, to the trailing edge where $q = q_U$. However, the requirement that the airfoil produce such a linear q(s) is not very crucial because the pressure distribution on the upper surface dominates the problem, and specification of q(s) over the entire airfoil contour may result in a geometry which is not physically meaningful. For example, the upper surface might cross over the lower surface at a point between the leading edge and the trailing edge. Thus, during the course of determining the geometry of the airfoil, liberty is taken with the pressure distribution on the lower surface in order to obtain a physically meaningful geometry. In regard to the pressure distribution on the upper surface, a slight modification also must be made. This modification is to change the abrupt pressure drop at the front stagnation point to a gradual one. Because an abrupt pressure drop at the front stagnation point corresponds to a leading edge of zero radius of curvature which is not suitable for operating the airfoil at various angles of attack, this modification is necessary. Knowledge about various types of airfoils will help in making a decision as to what is the most adoptable form of this modification.

III. DETERMINATION OF THE GEOMETRIES OF AIRFOILS WHICH PRODUCE THE OPTIMUM PRESSURE DISTRIBUTION

A. Review of Methods of Airfoil Design

1. Sato's Method and Weber's Method

The methods of designing airfoils with velocity specified along the airfoil surface fall into two categories. One is the method of conformal transformation and the other is the method of distribution of singularities. The most powerful method which belongs to the first category is the one developed by Sato.[4] The basic formulae used by Sato actually are those developed by Lighthill,[5] but Lighthill's method has the disadvantage that velocity must be specified in terms of closed form functions in order to be able to carry out the necessary integration. With the help of high speed computers, Sato's method allows a velocity distribution of any kind to be specified, and the integrations are carried out numerically. The expression for the velocity distribution is assumed in such a way that the front and the rear stagnation points can be treated separately. A well-behaved function $g(\theta)$ takes up the velocity distribution everywhere with the exception of the stagnation points and three constants A, B and τ which are embedded. These constants are determined by the function $g(\theta)$, the closure condition of the airfoil and the fact that flow field at infinity is a uniform one. Consequently, the resulting airfoil is always a closed curve and the disturbance dies out at large distances from the airfoil. The results are very accurate near the leading and the trailing edges where most other methods have difficulties. This is because the singularities caused by stagnation points are treated separately in an analytical way. The method is to be used on an

iterative basis in the sense that the computation must be repeated many times before a satisfactory geometry of the airfoil may be obtained. The reason of doing this is as follows. A set of initial values must be given to A, B and τ in order to obtain the function $g(\theta)$ from the specified velocity distribution. This $g(\theta)$ is to be used to obtain another set of A, B and τ which will give a closed curve as the airfoil geometry. Unless the initial set of A, B, and τ happens to hit the solution of the design problem, these two sets of A, B and τ will not be the same and the resulting airfoil will not produce the desired velocity distribution. The function $g(\theta)$, then, is modified in such a way that the airfoil geometry obtained in the next cycle will produce a velocity distribution which is closer to the desired one. This procedure is repeated until the specified velocity distribution is reached. Therefore, Sato's method always guarantees an airfoil which produces the desired velocity distribution to be obtained.

Turning to the method of distribution of singularities, one observes that the crudest one is the inverse of thin airfoil theory. Since large disturbances are not allowed in thin airfoil theory, airfoils with large thickness/chord ratios and/or large cambers which are operating at high angles of attack can not be obtained by this method. Modifications have been made by Weber[6] to include this capability by considering both first order and second order terms.

2. Method of Conformal Transformation and Method of Distribution of Singularities in Designing Multiple-Element Airfoils

When an airfoil of more than one element is to be designed, both Sato's and Weber's methods fail. Because Sato's method employs conformal

transformation, the reason why it fails for multiple-element airfoils is obvious. Take an airfoil of two elements as an example. The domain outside this airfoil is a triply connected one while the domain outside a single-element airfoil is a doubly connected one. Therefore, all the theories and formulae developed for the latter cease to be applicable to the former. Weber's method seems more likely to be applicable to multiple-element airfoil design. But, using a conventional airfoil with a slotted flap as an example, the angle of attack and camber of the flap are not properly defined and their contributions to the velocity distribution are difficult to identify. In view of the fact that no other methods of airfoil design are capable of treating airfoils consisting of more than one element, the necessity of developing a new method becomes clear.

The first method considered was the conformal transformation. The reason for proceeding in this direction was that Sato's method shows that single-element airfoils with satisfactory geometry which produce the desired velocity distributions can always be obtained by employing a conformal transformation and modifying the transformation function in a systematical way. As shown by Garrick,[7] the domain outside two closed contours can be transformed into the annular region between two concentric circles. Alternatively, a domain of rectangular shape may be obtained with the help of a logarithmic function. In this case, the two contours are mapped into two sides of the rectangle which are facing each other. Garrick performed this transformation on two NACA 4412 airfoils and computed the velocity distribution on the surface of each airfoil in the same fashion as Theodorsen computed the velocity distribution on the

surface of a single airfoil by transforming the airfoil into a cricle. Therefore, by inverting Garrick's method, geometries of two-element airfoils should be obtainable by specifying the velocity distribution along the boundaries of the annular region between the concentric circles. Based upon this concept, a set of formulae, which states the closure condition of each element of the two-element airfoil, was derived. Expressions for velocity distributions were the same as the one used by Sato. It was impossible to obtain the explicit formulae for computing the constants. Instead, all the six constants which are part of the velocity distribution and hence part of the transformation function appear implicitly in six integral relations. When the numerical calculations were carried out on a computer, it was found that a tremendous amount of time and work was required to find one set of constants. Since this method is to be used also in an iterative way, the time and work involved in computing several sets of constants make this treatment of the design problem formidable. As indicated by Garrick, the relative position of the two elements varies with the values of four other constants, and no study has been made as to how these values determine the relative position. Because of these two drawbacks, the method of conformal transformation was considered intractable in designing multiple-element airfoils. Next to be considered was the method of distribution of singularities.

The method of distribution of singularities was originally a method of computing the pressure distribution on the surface of a given airfoil. Singularities of unknown strengths such as sources, sinks, doublets or vortices are distributed inside the airfoil contour or on the airfoil surface. The strengths of these singularities are obtained by computing

the velocities induced by these singularities and requiring the tangency condition be satisfied. The surface pressure distribution is then computed from the strengths of these singularities. When this method is applied to solving a design problem, an iterative procedure is necessary. The starting point of this iterative procedure is an airfoil with arbitrary shape. The pressure distribution on the surface of this starting configuration is computed by the method of distribution of singularities. Then a modification of the geometry is performed according to how much the computed pressure distribution differs from the desired one. Generally, more than one modification is necessary and the iterative process continues until a satisfactory pressure distribution is achieved by the airfoil. At this stage, there are two questions which must be answered. One is how the pressure distribution on the surface of a given airfoil should be computed. The other is how to modify the geometry of the airfoil in such a way that the velocity distribution on the surface of the modified airfoil will be closer to the desired one than the previous one is. The answers to these two questions are presented in the following sections.

B. Methods of Computing Pressure Distribution on the Surface of a Given Airfoil

There are many methods of distribution of singularities available in the literature which compute the velocity distribution on the surface of a given airfoil. In the earlier methods, singularities are distributed inside the airfoil contour. The disturbances produced by the airfoil are considered to be composed of those due to thickness of the airfoil and those due to camber and angle of attack. Sources and sinks are used

to represent the former, and the latter are represented by vortices. In the newly developed methods, all the singularities are distributed on the airfoil surface, and the pressure distributions are computed by solving integral equations of different forms. The outstanding feature of these methods is that the airfoils under consideration can possess any geometry and any orientation relative to the free stream. Effects of thickness, camber and angle of attack do not have to be considered separately. As a general property and hence a limitation of the method of distribution of singularities, the fluid flow is considered to be incompressible and nonviscous.

Among all the new-fashioned methods, perhaps the best known is the method of Hess and Smith.[8] Although this method has gained such publicity that it almost becomes a standard method of computing velocity distribution on the surface of an airfoil in incompressible potential fluid flow, it has some drawbacks which have not been noticed by many people. There are two other methods which are very effective but not known to many people in this country. They were developed in Germany and one is by Martensen[9] and Jacob,[10] the other is by Oellers.[11] These three methods will be analyzed and compared with each other in the following subsections.

1. Hess-Smith's Method

In this method, the airfoil surface is replaced by a source sheet with strength $\sigma(s)$, where s is the distance measured along the airfoil surface. Considering the airfoil to be stationary, velocities induced by the source sheet are combined with the free stream velocity to satisfy the

tangency condition that there should be no velocity component normal to the airfoil surface. This concept results in a Fredholm integral equation of the second kind

$$2\pi\sigma(s) + \int_0^{s_T} \sigma(s') \frac{\partial}{\partial n} \ln r(s,s')ds' = F(s) \qquad (23)$$

where s_T denotes the trailing edge of the airfoil, $r(s,s')$ is the distance between two points represented by s and s', and $F(s)$ is a function related to onset flows. For a uniform free stream, $F(s) = -\vec{U}_\infty \cdot \vec{n}(s)$ where $\vec{n}(s)$ is the local outward unit normal vector. In this equation, the first term on the left hand side represents the normal velocity at point s induced by the local source $\sigma(s)$. The second term represents the normal velocity at point s induced by the remaining source sheet. When the geometry of an airfoil is given together with the direction of the free stream, both the right hand side of the equation and the kernel of the integral are known. Hence the equation can be solved for $\sigma(s)$. In principle, the equation may be solved by analytical methods such as Neumann series successive approximation. In practical application, however, numerical methods are appropriate. Based on this concept, the contour of the given airfoil is divided into N segments. The integral term in the integral equation may be written as

$$\sum_{j=1}^{N} \int_{s_j}^{s_{j+1}} \sigma(s') \frac{\partial}{\partial n} \ln r(s,s')ds'$$

where s_j and s_{j+1} are the end points of segment j. At this stage, Hess and Smith make the approximation that $\sigma(s)$ takes a constant value within each segment. This approximation will tend to be exact when N goes to infinity. With this approximation, the integral becomes

$$\sum_{j=1}^{N} \sigma_j \int_{s_j}^{s_{j+1}} \frac{\partial}{\partial n} \ln r(s,s')ds'$$

where σ_j is the constant value of $\sigma(s)$ in segment j. In order to carry out the integrations analytically and hence simplify the problem further, two more approximations are made. One is to approximate the curved segment j by a straight line joining the end points of segment j With this approximation, each integral may be evaluated for a specified point s regardless of the precise shape of the segment j. Since the coordinates of the end points of each segment must be known, a convenient choice of this point s would be the mid-point of the chord line of each segment. The second approximation is that the integral equation (23) is not to be applied on the airfoil surface. Instead, it will be applied at the mid-point of the chord line of each segment. Therefore, N equations may be obtained by applying equation (23) at N of these mid-chord points. This system of equations may be written in the form of

$$\sum_{j=1}^{N} K_{ij}\sigma_j = F_i , \quad i = 1,2,\ldots,N \tag{24}$$

where $F_i = -\vec{U}_\infty \cdot \vec{n}_i$ and $\vec{n}_i$ is the unit outward normal vector of chord i. K_{ij} is the abbreviation of

$$\int_{s_j}^{s_{j+1}} \frac{\partial}{\partial n_i} \ln r(s,s')ds'$$

where s denotes the mid-point of chord i and integration has been carried out along the chord j. When i equals j, the value of K_{ij} is 2π which is the coefficient of the first term on the left hand side of equation (23). Literally, K_{ij} represents the outward normal velocity at mid-point of chord i induced by a source sheet with uniform strength unity located at chord j. When the geometry of the airfoil is given in terms of the coordinates of N discrete points, the coefficient matrix K_{ij} can be computed. The right hand side is then determined once the free stream direction is given. Therefore, a solution σ_i can be obtained by solving this system of N simultaneous linear algebraic equations. This solution is an approximate solution to equation (23) evaluated at discrete points. Because the integration is carried out along the chord line of each segment in obtaining K_{ij} and equation (23) is actually applied at mid-chord points which are slightly off the airfoil surface, the segmentation of the airfoil surface should be made in such a way that segment size is smaller in the high curvature region and larger in the low curvature region of the airfoil surface. In other words, more segments are needed near the high curvature region in order to obtain better results. This does not imply that the segment can be made very large when a large portion of the airfoil surface is a straight line. The reason is that the variable $\sigma(s)$ will not be a constant even for a straight line portion of the airfoil surface. Hence the segment size must be kept small even for a straight line portion of the airfoil surface order that the first approximation made by Hess and Smith can be considered to be a good one.

With the solution to equation (24), the velocity tangent to the airfoil surface can be computed by combining the tangential component

of the free stream velocity and the tangential velocity induced by the source sheet. This surface velocity usually does not vanish at the trailing edge of the airfoil when the airfoil is generating a lifting force. Therefore, an additional set of σ_i must be superposed to the solution of equation (24) in order to insure that the fluid will flow off the trailing edge smoothly. This set of σ_i is obtained as the solution to a system of simultaneous linear equations with the same coefficient matrix K_{ij} appearing in equation (24) but with a different right hand side. The right hand side F_i for this purpose is the normal velocity at each midchord point induced by a vortex sheet with unit strength which has exactly the same location as the approximating source sheet. The solution to this system is a source sheet which will induce a tangential velocity on the airfoil surface which corresponds to the surface velocity distribution due to a unit circulatory flow around the airfoil. By combining these two sets of σ_i's and varying strength of the vortex sheet, one is able to satisfy the Kutta condition with a circulatory flow of strength Γ. This Γ essentially represents the circulation generated by the airfoil. With this Γ, the real tangential velocity V_T along the airfoil surface can be computed by combining the tangential component of uniform free stream, the tangential velocities induced by the two sets of σ_i's. Pressure distribution can then be obtained by computing the pressure coefficient from

$$C_p = 1 - \left(\frac{V_T}{U_\infty}\right)^2.$$

2. Martensen-Jacob's Method

Instead of replacing the airfoil surface by a source sheet, Martensen[9] uses a vortex sheet. By requiring that the strength of the vortex sheet be identical to the velocity distribution on the surface of an airfoil, Martensen was able to show that the interior of the closed vortex sheet must have zero velocity everywhere. In particular, the tangential velocity at every point on the inner side of the vortex sheet caused by the free stream and the vortex sheet should be zero. This result can be represented also by a Fredholm integral equation of the second kind

$$\frac{\gamma(s)}{2} - \frac{1}{2\pi}\frac{\partial}{\partial n}\int_0^{s_T} \gamma(s')\ln r(s,s')ds' = U_\infty \left(\frac{dx}{ds}\cos\alpha + \frac{dy}{ds}\sin\alpha\right) \qquad (25)$$

where $\gamma(s)$ is the strength of the vortex sheet and α denotes the free stream direction. This equation almost has exactly the same form as equation (23). The corresponding terms possess similar meaning except that the tangential velocities are considered in equation (25).

When solving equation (25), Martensen also replaces the integral by a summation, and hence a system of simultaneous equations is to be solved. However, when approximating the integral, the first law of the mean is used in contrast to the second law of the mean employed by Hess and Smith. When 2N control points are distributed along the airfoil surface, the resulting system of simultaneous linear equations can be written as

$$\sum_{j=1}^{2N} K_{ij}\gamma_j = 2Nw_i \ , \quad i = 1,2,\ldots,2N \tag{26}$$

where γ_j is the vortex strength at point j and

$$w_i = U_\infty[\dot{x}_i(\theta)\cos\alpha + \dot{y}_i(\theta)\sin\alpha]$$

$$K_{ij} = -\frac{(x_i-x_j)\dot{y}_i(\theta) - (y_i-y_j)\dot{x}_i(\theta)}{(x_i-x_j)^2 + (y_i-y_j)^2} \quad i \neq j$$

$$= -\sum_{\substack{i=1 \\ i\neq j}}^{2N} K_{ij} \qquad i = j.$$

The independent variable has been changed from s to θ where θ is the angular coordinate of the image of a control point when the airfoil is transformed into a circle. The control points on the airfoil surface are to be distributed in such a way that their images are equally spaced on the circle, and hence the interval over which the law of the mean is applied is $\frac{2\pi}{2N}$. Dots over x and y indicate derivatives with respect to θ. The identity $\sum_{i=1}^{2N} K_{ij} = 0$ comes from the fact that

$$\int_0^{s_T} \frac{\partial}{\partial n} \ln r(s',s)ds' = -\pi. \tag{27}$$

Equation (27) makes the solution $\gamma(s)$ of equation (25) non-unique and this character is carried over to the system of equations which replaces equation (25). Indeed, equation (26) is not a linearly independent system and the coefficient matrix K_{ij} has a rank of only 2N-1. The only degree of freedom of the system is annihilated by applying the Kutta condition.

The solution obtained is the velocity distribution on the airfoil surface. This is an advantage of this method when compared with Hess-Smith method. As previously stated, the direct solution to equation (24) is the source strength, and the surface velocity has to be obtained from this source sheet. However, Martensen's method does not give good results for thin airfoils with thickness/chord ratios less than 10%. The reason is that when the airfoil is thin, the control points on the upper and lower surfaces are very close to each other, and the vortices located there induce strong tangential velocities on each other. While this induced velocity decays very rapidly for points in the neighborhood of the control point, the first law of the mean assumes it to be a constant. Therefore, the computed result γ_j is not a good approximation to the true solution to equation (25). Jacob[10] modified Martensen's method by taking the limit of K_{ij} when i approaches j to be the value of K_{ii}. This gives

$$K_{ii} = N - \frac{1}{2} \frac{\dot{x}_i(\theta)\ddot{y}_i(\theta) - \dot{y}_i(\theta)\ddot{x}_i(\theta)}{\dot{x}_i(\theta)^2 + \dot{y}_i(\theta)^2} \quad .$$

Then the value of K_{ij} for control points directly facing each other, e.g., $i = 2N - j + 2$ for symmetrical airfoils, is obtained from $\sum_{i=1}^{2N} K_{ij} = 0$. This modification improves the results obtained from Martensen's method, but it places a restriction on how the control points are to be distributed over the airfoil surface. Also, it can cause a lot of inconvenience for airfoils such as those obtained by Liebeck and Ormsbee[1]

3. Oellers' Method

Oellers[11] developed a method to compute the pressure distribution on the surface of cascades of airfoils in tandem. The surface of each airfoil is replaced by a vortex sheet which must be a streamline. Instead of working with induced velocities, a method used by both Hess-Smith and Martensen-Jacob, stream functions are employed. The stream function for a uniform free stream is added to that of the vortex sheet, and the sum is set to be a constant on the airfoil surface. This requirement is represented by a Fredholm integral equation of the first kind

$$\psi = u_\infty y(s) - v_\infty x(s) - \frac{1}{2\pi}\int_0^{s_T} \gamma(s') \times \ell n\left\{\sinh^2 \frac{\pi[x(s)-x(s')]}{t} + \sin^2 \frac{\pi[y(s)-y(s')]}{t}\right\}^{1/2} ds'$$

where $u_\infty = U_\infty \cos\alpha$, $v_\infty = U_\infty \sin\alpha$, t is the spacing of the cascade and ψ is an unknown constant. When a single-element airfoil is under consideration, the kernel of the integral becomes $\ell n\, r(s,s')$ and the equation reads

$$\psi = u_\infty y(s) - v_\infty x(s) - \frac{1}{2\pi}\int_0^{s_T} \gamma(s')\ell n\, r(s,s')ds' \quad . \qquad (28)$$

To solve this equation for ψ and $\gamma(\varepsilon)$, the integral is again replaced by a summation using second law of the mean to approximate the integral. Dividing the airfoil surface into N segments and applying equation (28) at the mid-chord point of each segment results in a system of simultaneous linear equations of the form

$$\Psi = u_\infty y_i - v_\infty x_i + \sum_{j=1}^{N} K_{ij}\gamma_j \ , \ i = 1,2,\ldots,N$$

or

$$\sum_{j=1}^{N} K_{ij}\gamma_j - \Psi = v_\infty x_i - u_\infty y_i \ , \ i = 1,2,\ldots,N \qquad (29)$$

For an airfoil with the geometry given in cerms of coordinates of N points, the coefficient matrix K_{ij} may be computed and the right hand side of equation (29) is known once the free stream direction is given. However, there are N+1 unknown variables Ψ and γ_i's while only N equations are available. The solution is not unique. This degree of freedom is again removed by applying the Kutta condition at the trailing edge. Because a vortex sheet is used to represent the airfoil contour, the solution γ_i is the real tangential velocity on the airfoil surface. This is similar to Martensen-Jacob's method but Oellers' method is simpler due to less computation involved in obtaining the coefficient matrix.

4. Comparison of the Three Methods of Computing Pressure Distribution on the Surface of a Given Airfoil

Extensive investigations have been made in order to find various properties of the methods presented in the previous subsections and their applicability to solving the problem of airfoil design. The results are summarized as follows.

When applied to standard airfoils for which analytical expressions of pressure distribution are available, the Hess-Smith method always gives the correct value of circulation generated by the airfoil. This indicated that the pressure distribution computed by the Hess-Smith method is fairly close to the true value. However, the computed surface

velocity is found to be very sensitive to the coordinates of the control points on the airfoil surface which are used as the input of this method That is to say, the numerical values of the input coordinates have to be so accurate that they really do represent a smooth curve. A tiny error in the input coordinates can produce a wavy behavior of large amplitude in the computed surface velocity. This is illustrated in Figure 7. The upper half shows the trailing edge of a thin airfoil and the lower half shows the pressure distribution computed by the Hess-Smith method. An airfoil whose surface is not perfectly smooth will produce wavy pressure distribution along the airfoil surface but the amplitude computed by the Hess-Smith method is simply too large. This is attributed to the fact that this method chooses the velocity normal to the airfoil surface to be the variable to work with. Because airfoils are generally operating at moderate angles of attack and hence the free stream does not have large component normal to the airfoil surface, the consequence of using normal velocity as the variable is that a small absolute error introduced in computing the unit normal vector $\vec{n}_i$ by the non-exact input coordinates is a large relative error for the right hand side of equation (24). Therefore, by failing to represent the airfoil surface exactly with the input coordinates, the solution of equation (24) contains errors. These errors are especially large near the trailing edge of thin airfoils. This character of the Hess-Smith method makes it intractable to perform modifications of the geometry graphically when an airfoil design problem is to be solved. Alternatively, if the modification is to be accomplished by an iterative procedure programmed for a computer, the possibility is eliminated when one recalls that the tangential velocities

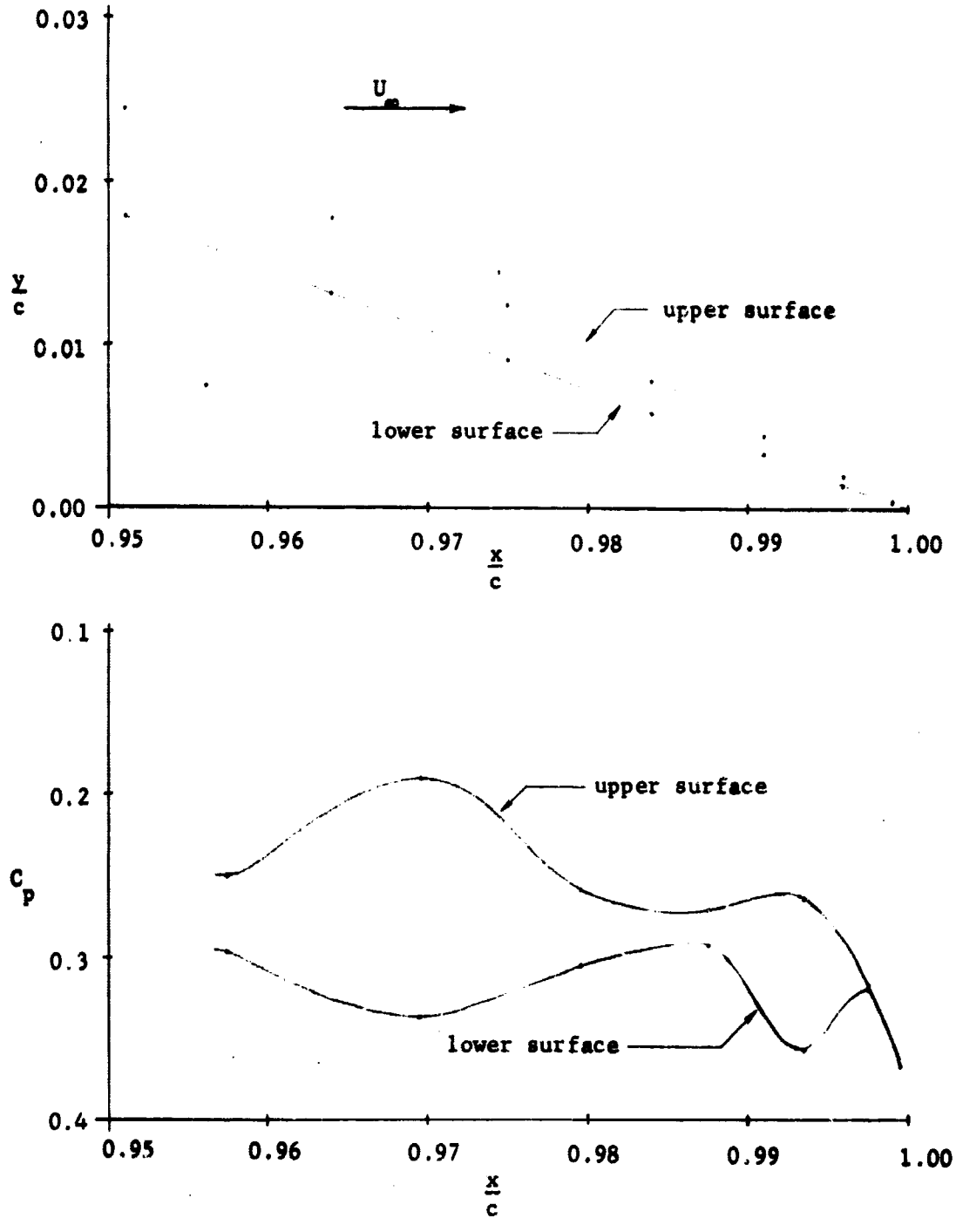

Figure 7. Sensitivity of pressure distribution computed from the Hess-Smith Method to the input coordinates.

on the airfoil surface have to be computed as those induced by all the discrete sources distributed on the approximated airfoil contour.

As noted by Jacob, Martensen's method does not give accurate results for thin airfoils. This drawback has been improved by Jacob by taking the steps described in Subsection III.B.2. However, this modification restricts the manner in which control points are to be distributed on the airfoil surface. As will be seen in the next chapter, all the airfoils which generate optimum pressure distributions have a sharp trailing edge with which a thin aft-part is inevitably associated. Therefore, a modification to the Martensen-Jacob method has been made during the course of this study in order that thin arifoils may be treated and no generality of how to distribute control points will be lost. The modification is to approximate the integral by using the second law of the mean instead of the first law of the mean. In other words, the scheme by which K_{ij} is computed in the Hess-Smith method is applied to equation (25). It is found that this modification serves the purpose of fulfilling the requirements described above, but the circulation generated by the airfoil is smaller than the one computed by the Hess-Smith method. Further investigation reveals the fact that the influence of local curvature on the induced velocity has been ignored when the coefficient matrix is obtained by carrying out the integration along the chord line of each segment instead of along the airfoil surface which is usually curved. This approximation did not bother Hess-Smith's results but the effects on the solution of equation (25) are far more than would be expected. The reason is a very interesting one: The diagonal elements of the coefficient matrix of the integral equation (23) have a positive

sign while those of the integral equation (25) have a negative sign. With everything else the same, this difference makes the coefficient matrix of equation (24) a diagonally dominated one while that of equation (26) is an almost singular one. When one uses the terminology of numerical analysis, the former is a well-conditioned matrix and the latter is an ill-conditioned one. Hence by neglecting the local curvature, a more severe consequence appears in Martensen-Jacob's results than in Hess-Smith's results. After the curvature effect is taken into consideration, the circulation computed by Martensen-Jacob's method increases, but it is still smaller than the value obtained by Hess-Smith's method. On the other hand, because it is the vortex sheet and tangential velocities which are considered by Martensen and Jacob, the computed results are not very sensitive to the inaccuracies of input coordinates. Small absolute errors introduced by non-exact coordinates in computing tangential vectors produce small relative errors for the right hand side of equation (26). Thus, wavy pressure distributions will be obtained when non-exact coordinates are used as input, but this is what should be expected. The wavy pressure distribution computed by the Hess-Smith method for a same set of coordinates is too exaggerated to be realized in real fluid flow. Hence the modified Martensen-Jacob method can be used in designing airfoils by an iterative procedure when modifications of geometry are to be made graphically. Also, the explicit appearance of surface velocity $\gamma(s)$ in the integral equation makes it possible that, when applied to airfoil design, a systematical way of modifying the geometry may be established and performed on a computer.

There are no references which give the pressure distributions along the surface of single-element airfoils computed by Oellers' method, but the numerical examples which have been worked out during the course of this study show that Oellers' method possesses many favorable characteristics. First, the computed surface velocities are relatively insensitive to inaccuracies of the input coordinates. This is attributed to the fact that the right hand side of the system of simultaneous equations (29) contains only the coordinates of the airfoil while derivatives must be computed both in the Hess-Smith method and the Martensen-Jacob method. Because computing derivatives numerically always causes a loss of accuracy, the results obtained by using Oellers' method are expected to have higher precision than the other two methods. Second, the circulation generated by the airfoil is found to be almost the same as the one computed by the Hess-Smith method. The word 'almost' is used here because all the numerical results are approximations to the real solution to the integral equation employed. Therefore, an identity of the results obtained from different approximations is almost impossible to achieve. The pressure distributions on the surface of standard airfoils are found to be very close to those obtained by analytical methods. This is true whether the airfoil is thick or thin or whether it has a rounded trailing edge or a sharp one. Third, the time consumed in computing the velocity distribution is less than that of any of the other methods. This is attributed to the simplicity of the kernel of integral equation (28). This characteristic is very important because the computation of surface velocity must be repeated many times during an iterative procedure of airfoil design.

These three characteristics, plus the fact that surface velocity $\gamma(s)$ appears explicitly in the integral equation, make the Oellers' method undoubtedly the appropriate tool to be used in airfoil design.

C. A New Method of Two-Dimensional Airfoil Design

As indicated in the previous sections, the problem of multiple-element airfoil design can be solved best by an iterative procedure in which the geometry of a starting airfoil undergoes modifications until the surface pressure distribution computed by a reliable method agrees with the desired one. The most reliable method of computing pressure distribution on the surface of an airfoil with given geometry has been found to be the one by Oellers while the modification of starting geometry has yet to be studied. Since the modification should be made according to how the computed velocity distribution differs from the desired one in order that the procedure converges to the desired answer, some means must be found by which the modified coordinates of the starting airfoil can be related to the desired velocity distribution. When the equation considered by Oellers in computing the surface velocity of an airfoil is recalled,

$$\psi = u_\infty y(s) - v_\infty x(s) - \frac{1}{2\pi}\int_0^{s_T} \gamma(s')\ln r(s,s')ds' \qquad (28)$$

one can see clearly that this is the appropriate relation between surface velocity $\gamma(s)$ and coordinates (x,y). In order to compute the pressure distribution on the surface of an airfoil, the coordinates of the airfoil may be normalized with respect to the chord length for the purpose of convenience. With this normalization made and approximately one

hundred control points distributed along the airfoil surface, the coefficient matrix K_{ij} obtained by approximating the integral in equation (28) is found to possess an excellent property. That is: most elements of K_{ij} are of order 10^{-3}, some of them are of order 10^{-2} and only a few are of order 10^{-1}. Therefore, if the equation is rewritten as

$$u_\infty y(s) - v_\infty x(s) = \psi + \frac{1}{2\pi}\int_0^{s_T} \gamma(s')\ln r(s,s')ds'$$

which can be replaced by

$$u_\infty y_i - v_\infty x_i = \psi - \sum_{j=1}^{N} K_{ij}\gamma_j \ , \ i = 1,2,\ldots,N,$$

the change of the summation term will not be large if each γ_i is changed by an amount of order one. This nice characteristic of the coefficient matrix forms the foundation upon which an iterative method of designing airfoils is based.

The method starts from a computation of velocity distribution along the surface of an airfoil. The geometry of the airfoil is an arbitrary one and it is given in the form of a set of coordinates. With this set of coordinates and a given free stream direction, the surface velocity can be obtained by solving the simultaneous linear equations

$$\sum_{j=1}^{N} K_{ij}\gamma_j - \psi = v_\infty x_i - u_\infty y_i \ , \quad i = 1,2,\ldots,N \qquad (29)$$

for γ_j's and ψ. This surface velocity $\gamma_j^{(0)}$ generally does not agree with the desired distribution because the coordinates represent merely an arbitrary airfoil. Hence the coordinates need to be changed in order to obtain the desired velocity distribution. At this time, equation (29) is

satisfied by the coordinates (x,y), the K_{ij} from this set of coordinates, the free stream direction and the computed $\gamma_j^{(0)}$'s, ψ. This identity will be destroyed when the computed $\gamma_j^{(0)}$ is replaced by the desired velocity $\gamma_j^{(d)}$. If the desired velocities $\gamma_j^{(d)}$ are kept there and an attempt is made to change the values of x,y in such a way that equation (29) is again satisfied, it would mean that an airfoil which produces the desired velocity distribution has been obtained, and this airfoil is represented by these new coordinates. In doing so, u_∞ and v_∞ may be kept unchanged. $\gamma_j^{(d)}$ is the desired value and it causes no trouble. Now, the equations are to be satisfied by varying x, y, ψ and K_{ij} while K_{ij} is strictly determined by (x,y). This puts too many constraints on the effort of making attempts to satisfy equation (29). Thus, an alternative approach is taken in which the coordinates of the airfoil which produces the desired velocity distribution are to be obtained by making several modifications to the original airfoil instead of one modification. The first step in achieving this is to retain the value of K_{ij} which corresponds to the original (x,y). The reason for doing so is that K_{ij} consists of N^2 elements. Each element has a different value, and it is impossible to find correct values for all the elements in order to satisfy equation (29). Now, the summation $\sum_{j=1}^{N} K_{ij}\gamma_j$ will have two values not much different from each other whether the γ_j is the desired velocity distribution or the one computed for the original airfoil. Therefore, it is to be expected that only small changes of x, y and ψ are needed to restore the identity of equation (29) after $\gamma_j^{(0)}$'s are replaced by $\gamma_j^{(d)}$'s. Since the goal is to change values of x and y, ψ is assumed to be unchanged and its original value is retained. At this point, the

situation is that the left hand side of equation (29) has been computed using the original values of K_{ij} and desired values of γ_j's. u_∞ and v_∞ are unchanged and the values of x and y are to be found such that the identity can be restored. Since N equations can uniquely determine only N variables, either x or y must be forced to take its original value. A study of Figure 8 will help in making this decision. In this figure, two airfoils are shown immersed in a common free stream. These two airfoils have entirely different angles of attack, thickness distributions and camber distributions. The only thing they have in common is that they span the same lengths in x direction. If the geometry of an airfoil is represented by a set of control points which are the intersections of the airfoil contour and the family of vertical lines shown in the figure, the geometry of one airfoil can be obtained simply by moving the control points of the other airfoil along these vertical lines. In other words, the geometrical characteristics of an airfoil can be completely changed by changing the y coordinates of the control points. Therefore, in restoring the identity of equation (29), the x values are assumed to have the original values. The system, then, contains N y-values to be determined from N equations. The solution to this system is easy and the y-values obtained will be designated by $y^{(1)}$. This $y^{(1)}$ together with the unchanged x-values actually represent the control points of an airfoil which would produce the desired velocity distribution if the coefficient matrix K_{ij} remained unchanged during the change of y-values. Because K_{ij} is completely determined by (x,y), the new airfoil represented by $(x,y^{(1)})$ will have a different coefficient matrix, $K_{ij}^{(1)}$, and hence the desired velocity distribution will not be realized. However, since

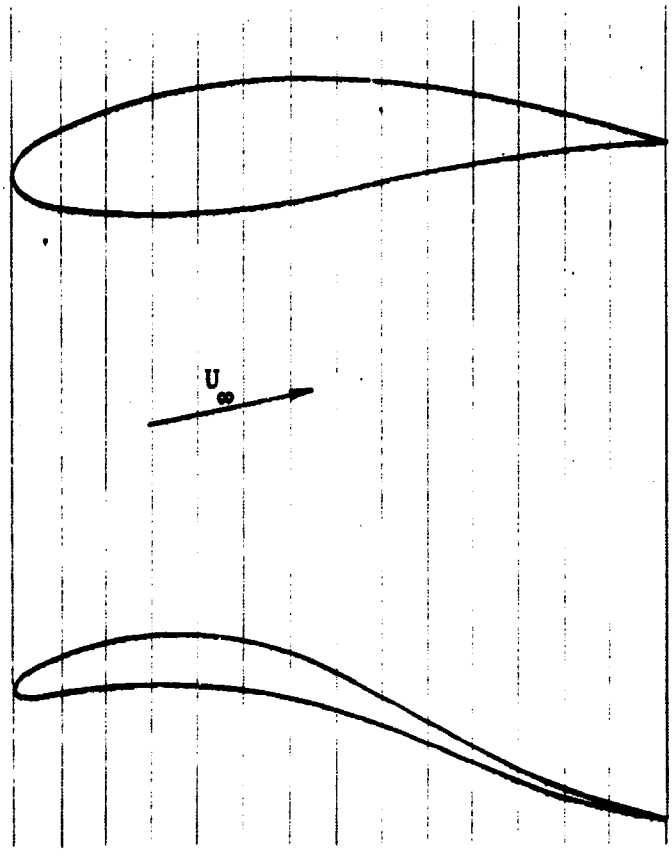

Figure 8. Variation of characteristics of a given airfoil by moving control points along vertical lines.

the difference $y_i - y_i^{(1)}$ is merely

$$\frac{1}{u_\infty} \sum_{j=1}^{N} K_{ij}[\gamma_j^{(d)} - \gamma_j^{(0)}]$$

which has been found to be small, the change in K_{ij} is to be expected to be small also. Hence the velocity distribution on the surface of this new airfoil is not much different from the desired distribution $\gamma_j^{(d)}$. Up to this point only one iteration has been completed. The geometry of this new airfoil can be modified again by changing the $y^{(1)}$ values by an amount

$$\frac{1}{u_\infty} \sum_{j=1}^{N} K_{ij}^{(1)}[\gamma_j^{(1)} - \gamma_j^{(d)}] .$$

The velocity $\gamma^{(2)}$ along the airfoil surface which is now represented by $(x,y^{(2)})$ is expected to be closer to $\gamma^{(d)}$ than $\gamma^{(1)}$ and $\gamma^{(0)}$ because the difference $y_i^{(2)} - y_i^{(1)}$ is smaller than $y_i^{(1)} - y_i$ in absolute value. Therefore, an iterative scheme has been established to obtain the geometry of an airfoil with velocity distribution specified along the airfoil surface. As will be seen in Chapter V, certain precautions must be taken when specifying the velocity distribution in order that a satisfactory airfoil may be obtained. For the examples presented in Chapter IV, the convergence of this iterative process was found to be fairly rapid. For clarity, the procedure can be formally stated as follows:

(i) Choose one of the standard airfoils as the starting configuration. Either Joukowski airfoils or NACA airfoils may be used because standard formulae are available to compute the coordinates of the

control points distributed along the airfoil contour. More control points are needed in high curvature regions in order to obtain accurate results. The coordinate system is to be oriented in such a way that the chord of the airfoil is parallel to the x-axis, and a free stream direction should be chosen. For a normalized chord length, one hundred control points were found to be satisfactory for the examples computed in this study.

(ii) With the control points chosen in (i), compute the surface velocity $\gamma_j^{(0)}$ by Oellers method.

(iii) Compare the computed velocity distribution with the desired one. Replace those γ_j's which are not desired by the desired values and evaluate

$$\sum_{j=1}^{N} K_{ij}\gamma_j \quad .$$

(iv) Obtain the y-coordinates of the modified airfoil from

$$y_i^{(m)} = \frac{1}{u_\infty}\left[v_\infty x_i + \psi^{(m-1)} - \sum_{j=1}^{N} K_{ij}^{(m-1)}\gamma_j^{(d)}\right] \qquad (30)$$

where superscripts (m) and (m-1) denote the sequence of iteration and superscript (d) denotes the word 'desired'.

(v) Compute the velocity distribution along the surface of this modified airfoil by Oellers method and return to (iii).

(vi) The repetition of steps (iii), (iv) and (v) is to be stopped when the velocity distribution obtained in (v) is satisfactorily close to the desired distribution.

The principle of this new method of airfoil design is not complicated, but some difficulties are encountered when an exercise of the design procedure is carried out. This will be seen in Chapter V.

For the purpose of demonstration and simplicity, the new method of airfoil design has been stated for problems of designing single-element airfoils. The entension to the problem of designing multiple-element airfoils is immediate. The appearance of several auxiliary elements in the flow field, in addition to the main element, simply adds more integral terms to equation (28), and the value of stream function ψ will be different for different elements. Therefore, equation (28) may be rewritten as a system of equations

$$\psi_p = u_\infty y_p(s_p) - v_\infty x_p(s_p) - \frac{1}{2\pi} \sum_{q=1}^{n} \int_0^{s_{T_q}} \gamma_q(s'_q) \ln r(s_p, s'_q) ds'_q,$$

$$p = 1,2,\ldots,n$$

where subscripts p and q denote the airfoil elements p and q respectively, and the system is assumed to consist of n elements. If the control points of each element are numbered in such an order that they all start from the trailing edge and go around the contour of each element in the same direction, a system of simultaneous linear equations can be written as

$$\sum_{j=1}^{N_T} K_{ij}\gamma_j - \psi_m = v_\infty x_i - u_\infty y_i , \qquad i = 1,2,\ldots,N_T \qquad (31)$$

where subscripts i and j denote the control points i and j respectively, N_T is the total number of control points and subscript m denotes the m-th element. There are n unknown ψ_m's and N_T unknown γ_j's to be solved,

but only N_T equations are available. This n degrees of freedom will be removed when the Kutta condition is applied at the trailing edge of each element. Therefore, the procedures of designing multiple-element airfoils are identical to the ones for designing single-element airfoils except that equation (31) should be used instead of equation (29).

It is important to point out that although this new method of airfoil design is powerful in the sense that the starting geometry does not have to produce a velocity distribution which is very close to the desired one in order to achieve a converging iterative process, there is a disadvantage in the way the airfoil geometry is modified. As stated in step (iv), the geometry of the airfoil is modified by changing the y-coordinates of control points. This modification can entirely change the character of a single-element airfoil. But, when multiple-element airfoils are under consideration, this method is not capable of making all the modifications permitted by the existing degrees of freedom. This is because each element ought to be able to move freely relative to the others during the modification while step (iv) only allows motions in the y-direction. Therefore, the relative position in x-direction is fixed once a starting configuration is given. This disadvantage, as will be seen in Chapter V, results in a possibility that an airfoil which produces the desired velocity distribution may not be obtained. Nevertheless, the necessary change of relative positions in x-direction still can be made by artificial means because the disadvantage described above exists only when the systematic steps (i)--(v) are to be programmed for a computer and the coordinates of control points are to be changed by the machine.

D. Selection of Parameters in Designing Two-Element Optimum Airfoils

As stated in Section II.B, the parameters which specify the optimum pressure distribution are the trailing edge velocity and Reynolds number Re_0. Because a non-zero trailing edge velocity is necessary to avoid an airfoil of infinite chord length, a convenient choice would be $q_U = 1$. Namely, the velocity at trailing edge is the same as free stream velocity. This choice is made for all the airfoils generated in this research and hence only different values of Re_0 need to be considered. As can be seen in Stratford's derivations, Re_0 specifies the boundary layer characteristics at x_0 and hence the zero skin-friction pressure distribution. In the variational problem, with trailing edge velocity fixed at $q_U = 1$, Re_0 determines the peak velocity, the extent of peak velocity plateau and the chord length which corresponds to a specified free stream velocity. Hence, to design a single-element optimum airfoil, an appropriate value of Re_0 must be chosen according to the desired free stream velocity and chord length. The exact value of lift coefficient is not known until the iterative process is terminated because the velocity distribution along the lower surface does not have a definite specification for the reason stated in Section II.C. For single-element airfoils, a given velocity distribution on the upper surface can be achieved by different airfoils having appropriate combinations of angle of attack, camber distribution and thickness distribution. Any one of these airfoils may be considered to be the solution to the optimization problem. However, the final decision as to which one is best suited for practical utilization depends on other criteria such as structural requirement, performance at various angles of attack, etc.

When two elements are present in the system, things are more flexible. To avoid unnecessary complexity, the requirement $q_U = 1$ is posed at the trailing edge of both elements. A value of Re_0 needs to be specified for each element and they depend only on the desired chord length of each element. With this information, the pressure distribution can be specified, and the iteration can start from an arbitrary configuration. In addition to the geometrical characteristics possessed by single-element airfoils such as angle of attack, camber distribution and thickness distribution, two-element airfoils have one more, namely, the relative position of two elements. With the velocity distribution specified definitely only on the upper surface of each element, there are many airfoils which can be considered as the solution to the optimization problem. These airfoils all produce the desired velocity distribution on the upper surface of each element, but they will have different angles of attack, different thickness and/or camber distributions of each element and different relative positions between the two elements. Once again, structural aspects and aerodynamic behaviors at various attitudes play important roles in determining which airfoil is optimum in the $C_{L_{max}}$ sense and utilizable in constructing wing sections.

IV. EXAMPLES

During the development of the new method of airfoil design, a two-element airfoil was considered in which one element was placed near the trailing edge of the other. This simulates the conventional wing which possesses a slotted flap as the high lift device. Values of 5×10^6 and 10^6 were chosen for Re_0 because they give a chord ratio approximately 4. After the development of the method was completed, another two-element airfoil was generated with $Re_0 = 10^7$ and 2×10^6. With these two sets of Reynolds numbers, different relative positions were assigned to both airfoils in order to investigate the effects of relative position of the two elements. The results are presented in graphic form in Figures 9 to 18. Both geometry and pressure distribution are shown in the figures. Free stream direction is at an angle of 11.25° measured from positive x-axis. Each figure shows the result obtained by completing ten iterations of the procedure described in Section III.C. The time consumed by an IBM computer model 360/75 were approximately 187 seconds and the figures were drawn by the Calcomp Plotter. Since the Plotter only draws straight lines, symbol x indicates where C_p was computed, and Lagrangian interpolation was employed in plotting the airfoil contours.

In addition to the two-element airfoils, two single-element airfoils were generated. Values of 5×10^6 and 10^7 were chosen for Re_0 in order to compare the geometries with two-element airfoils. Sato's method was employed and the resulting airfoils were found to possess highly curved leading edges. Also, the thickness ratio was found to be less than 9%. Shown in Figure 19 is the airfoil for $Re_0 = 5 \times 10^6$ together with three

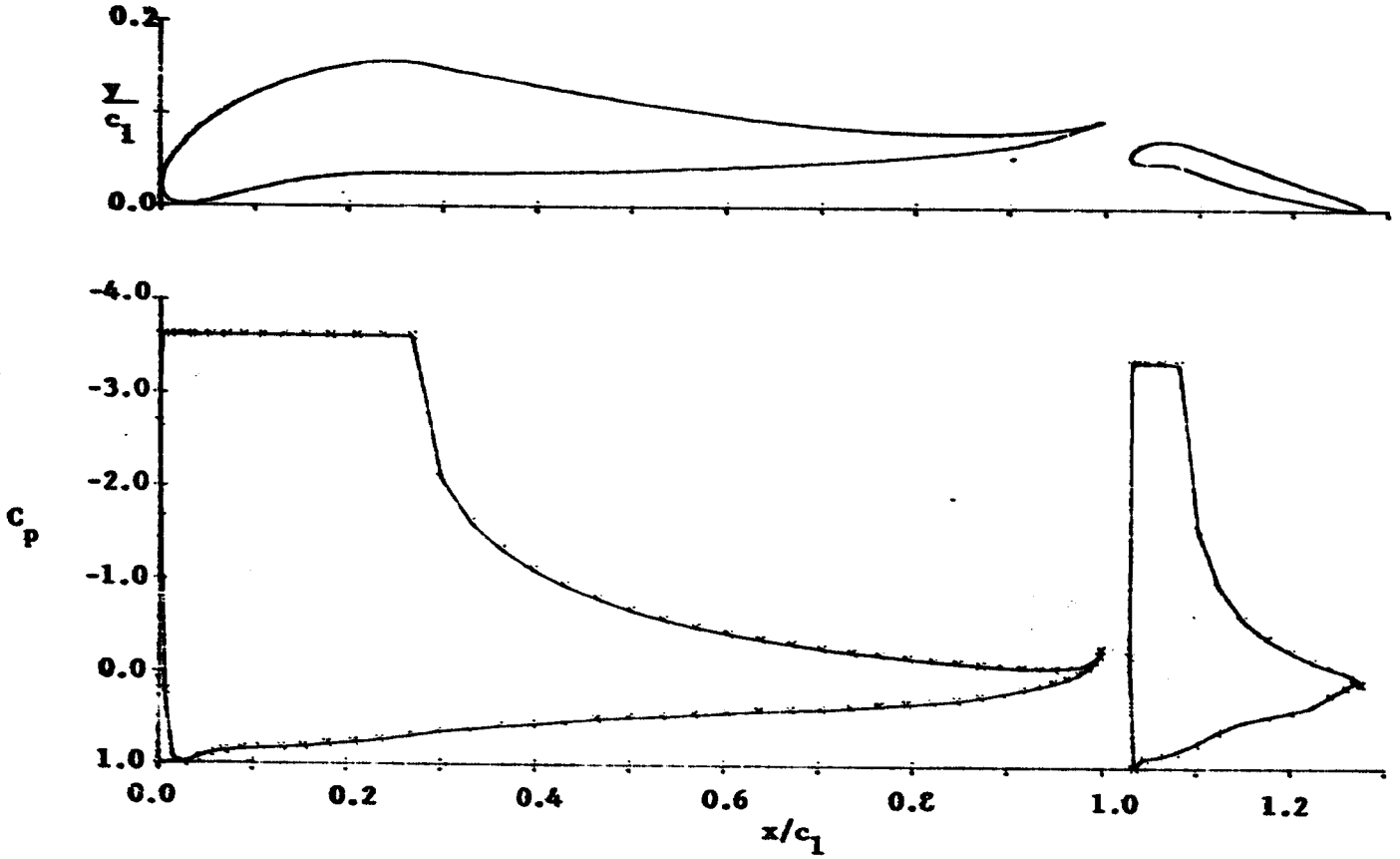

Figure 9. Geometry and pressure distribution of two-element optimum airfoil for $Re_{01} = 5 \times 10^6$ and $Re_{02} = 10^6$, $C_L = 2.38614$.

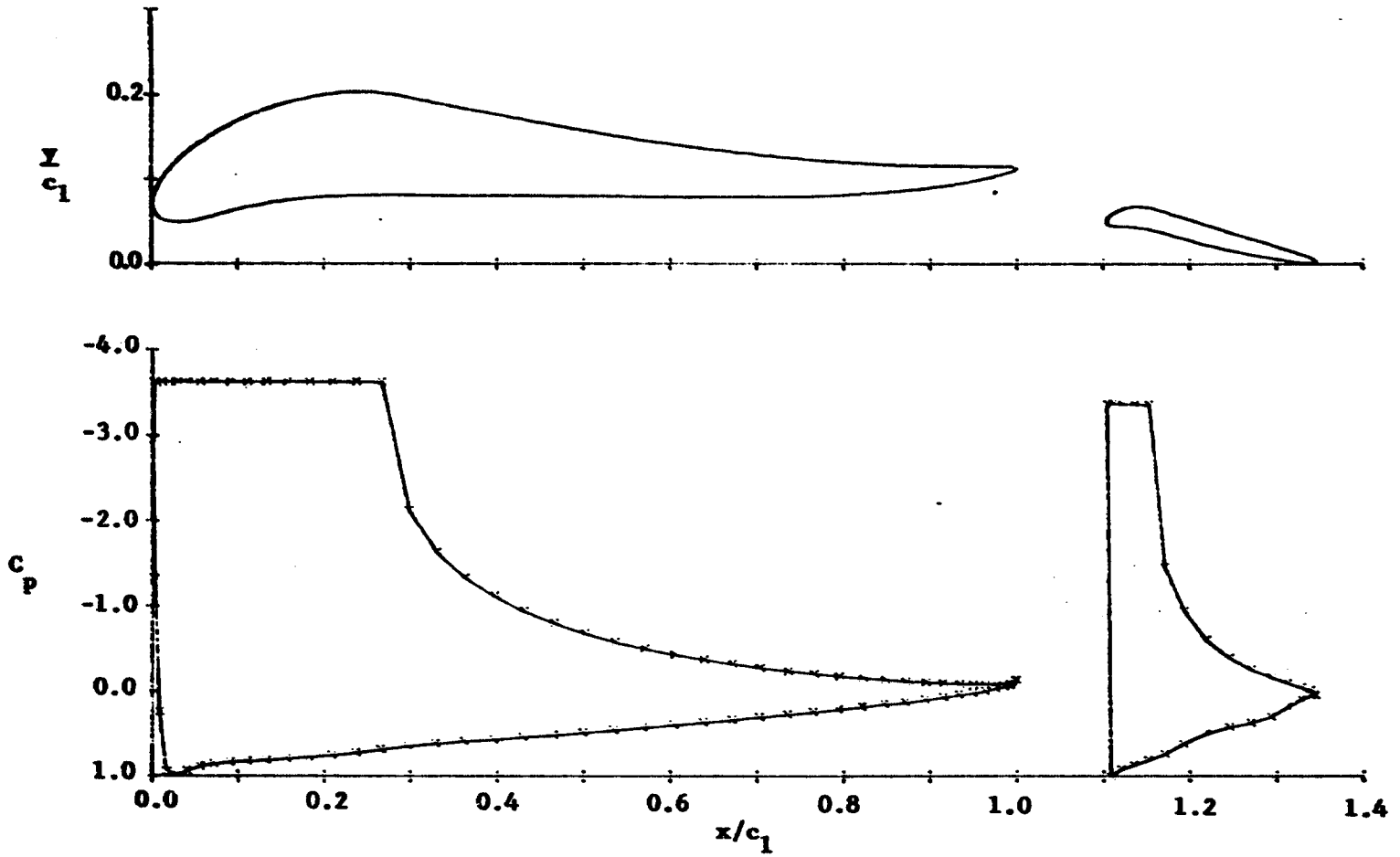

Figure 10. Geometry and pressure distribution of two-element optimum airfoil for $Re_{01} = 5 \times 10^6$ and $Re_{02} = 10^6$, $C_L = 2.32828$.

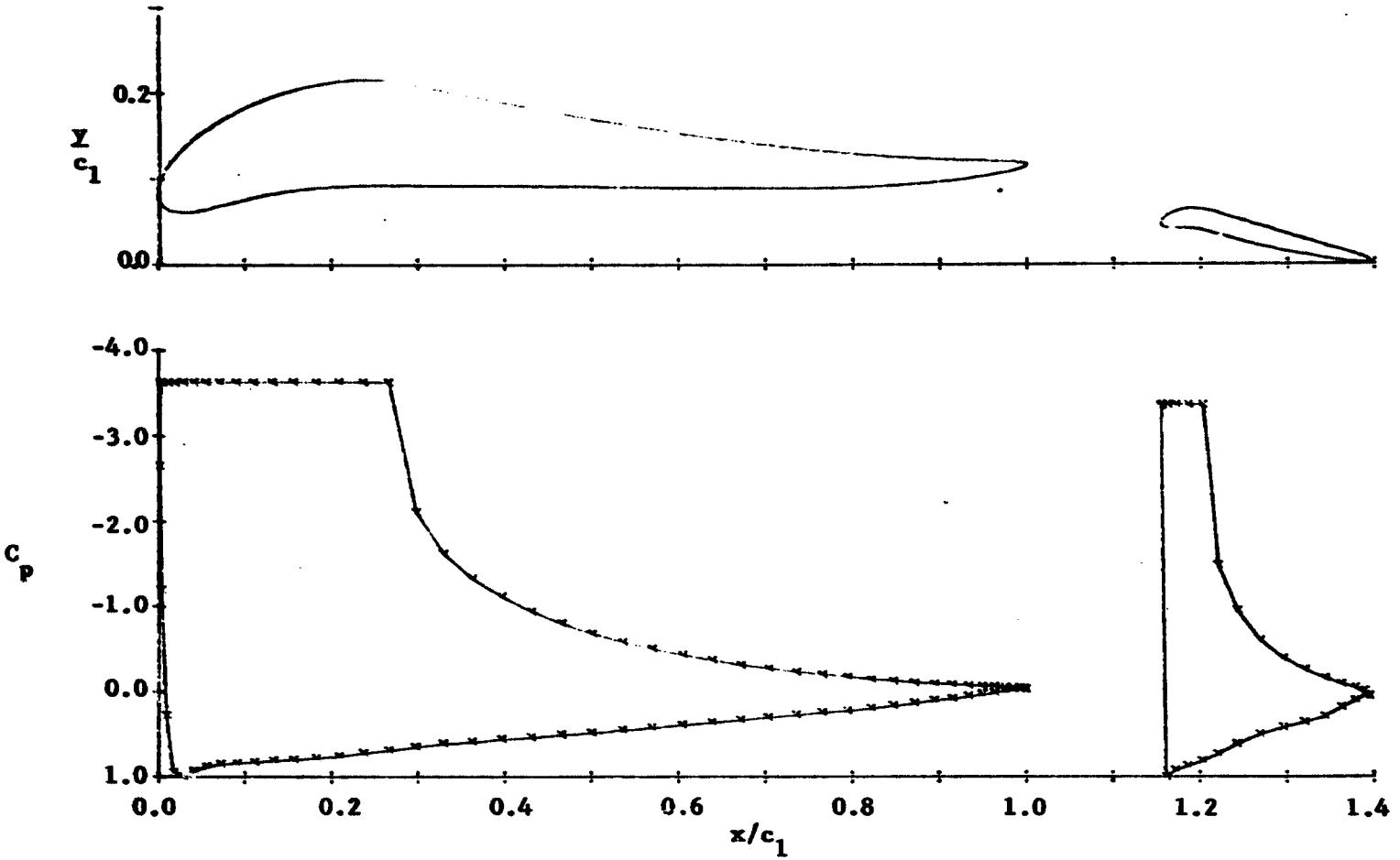

Figure 11. Geometry and pressure distribution of two-element optimum airfoil for $Re_{01} = 5 \times 10^6$ and $Re_{02} = 10^6$, $C_L = 2.32202$.

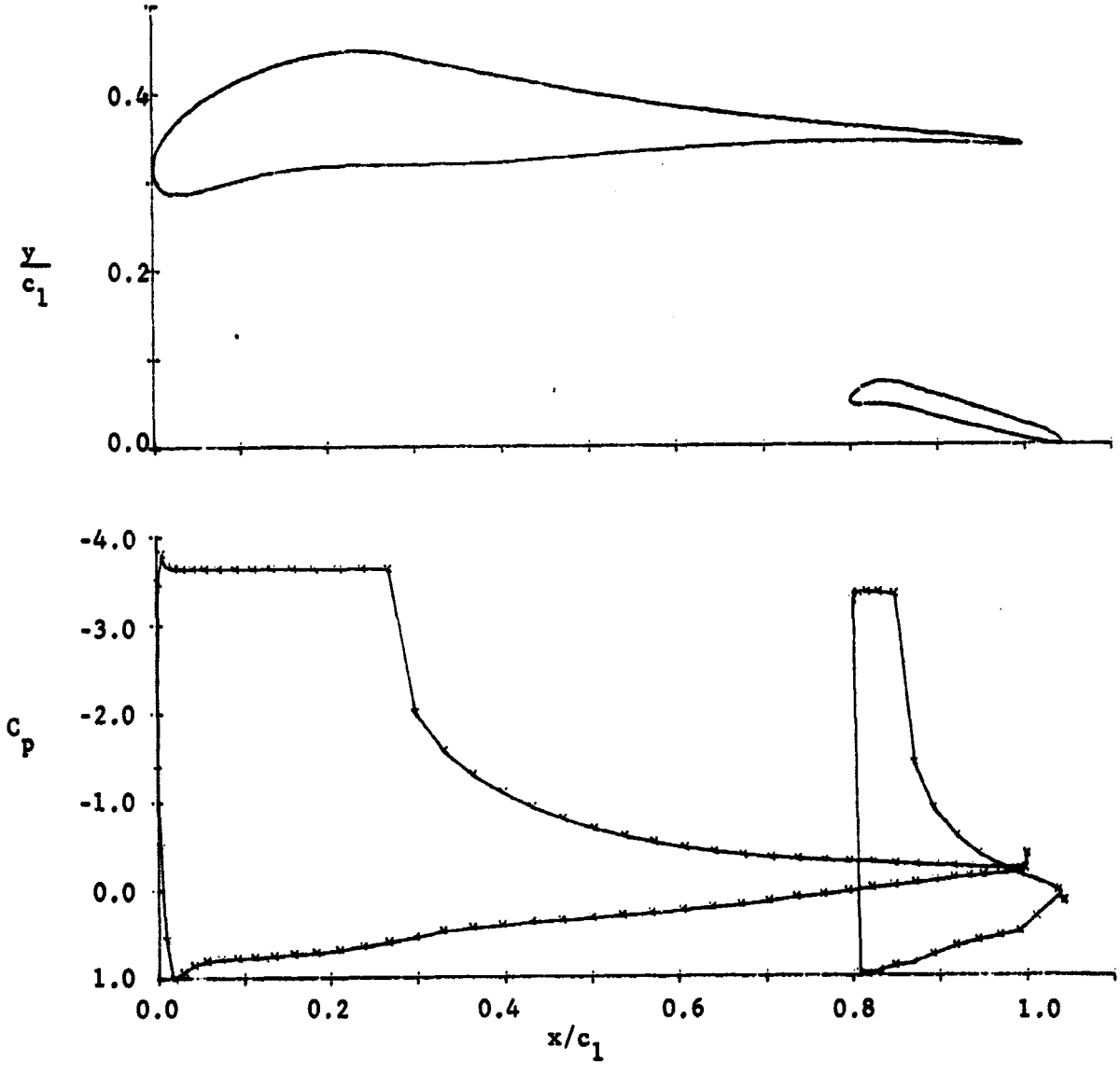

Figure 12. Geometry and pressure distribution of two-element optimum airfoil for $Re_{01} = 5 \times 10^6$ and $Re_{02} = 10^6$, $C_L = 2.27442$.

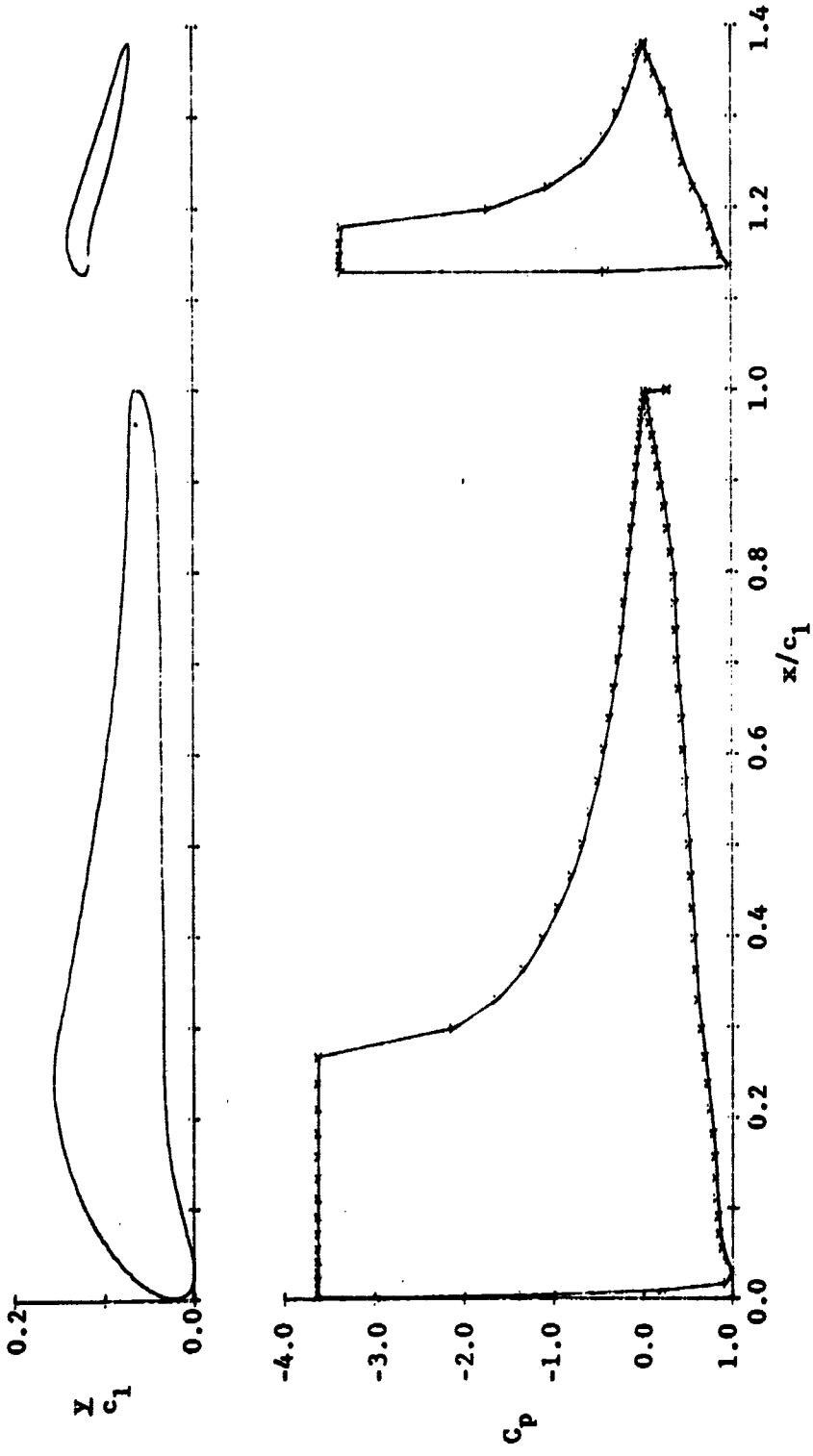

Figure 13. Geometry and pressure distribution of two-element optimum airfoil for $Re_{01} = 5 \times 10^6$ and $Re_{02} = 10^6$, $C_L = 2.39382$.

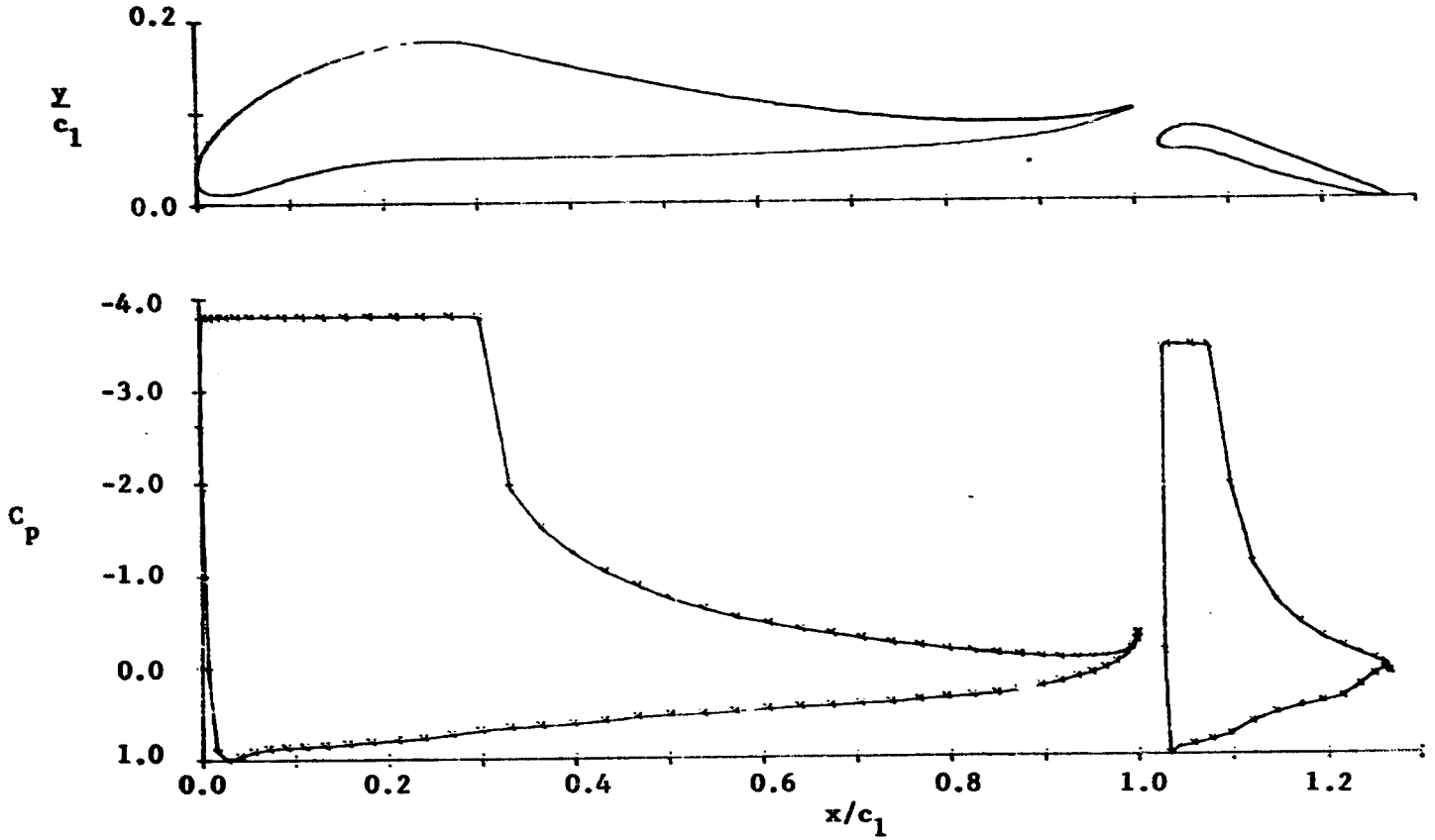

Figure 14. Geometry and pressure distribution of two-element optimum airfoil for $Re_{01} = 10^7$ and $Re_{02} = 2 \times 10^6$, $C_L = 2.58064$.

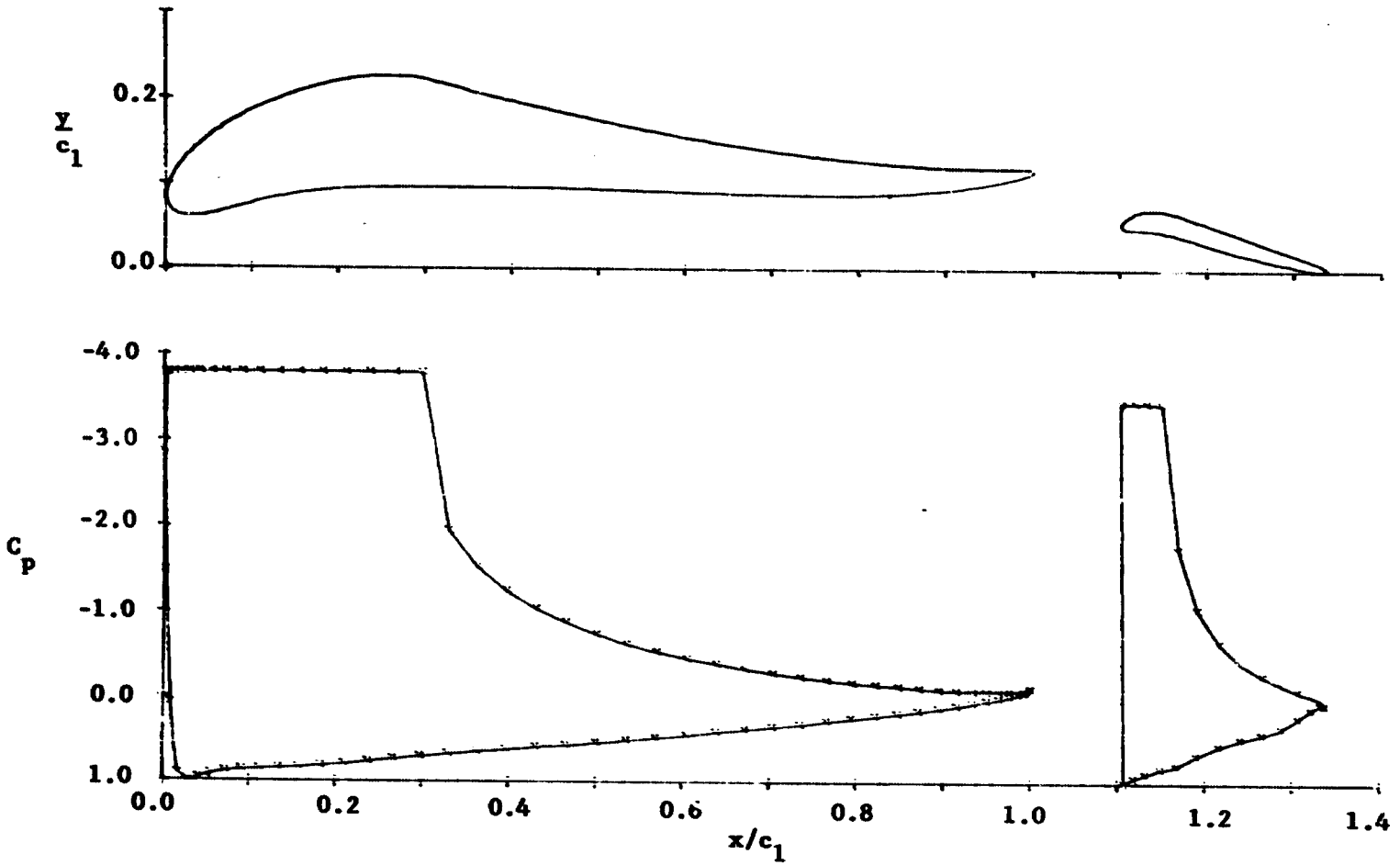

Figure 15. Geometry and pressure distribution of two-element optimum airfoil for $Re_{01} = 10^7$ and $Re_{02} = 2 \times 10^6$, $C_L = 2.51508$.

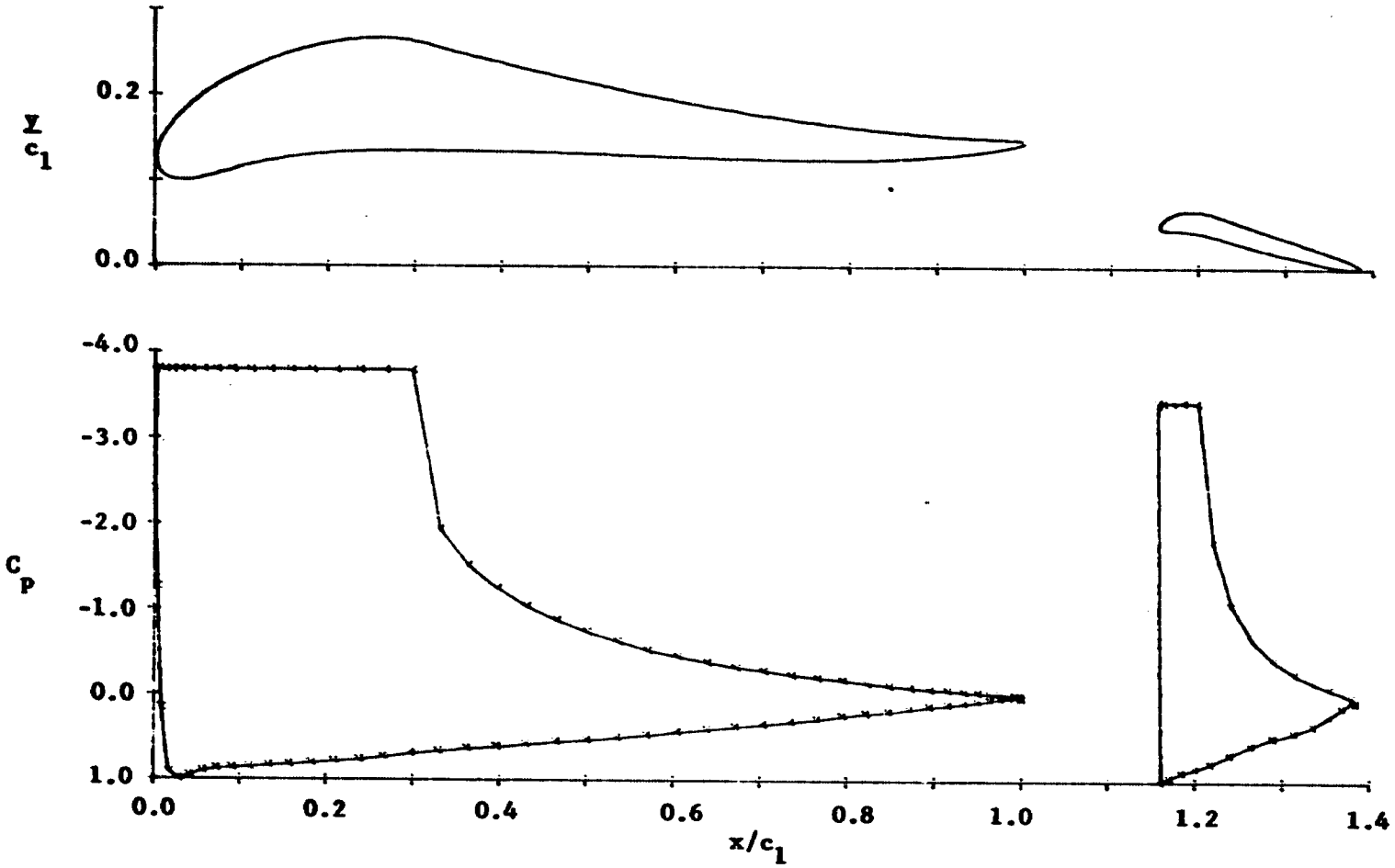

Figure 16. Geometry and pressure distribution of two-element optimum airfoil for $Re_{01} = 10^7$ and $Re_{02} = 2 \times 10^6$, $C_L = 2.49528$.

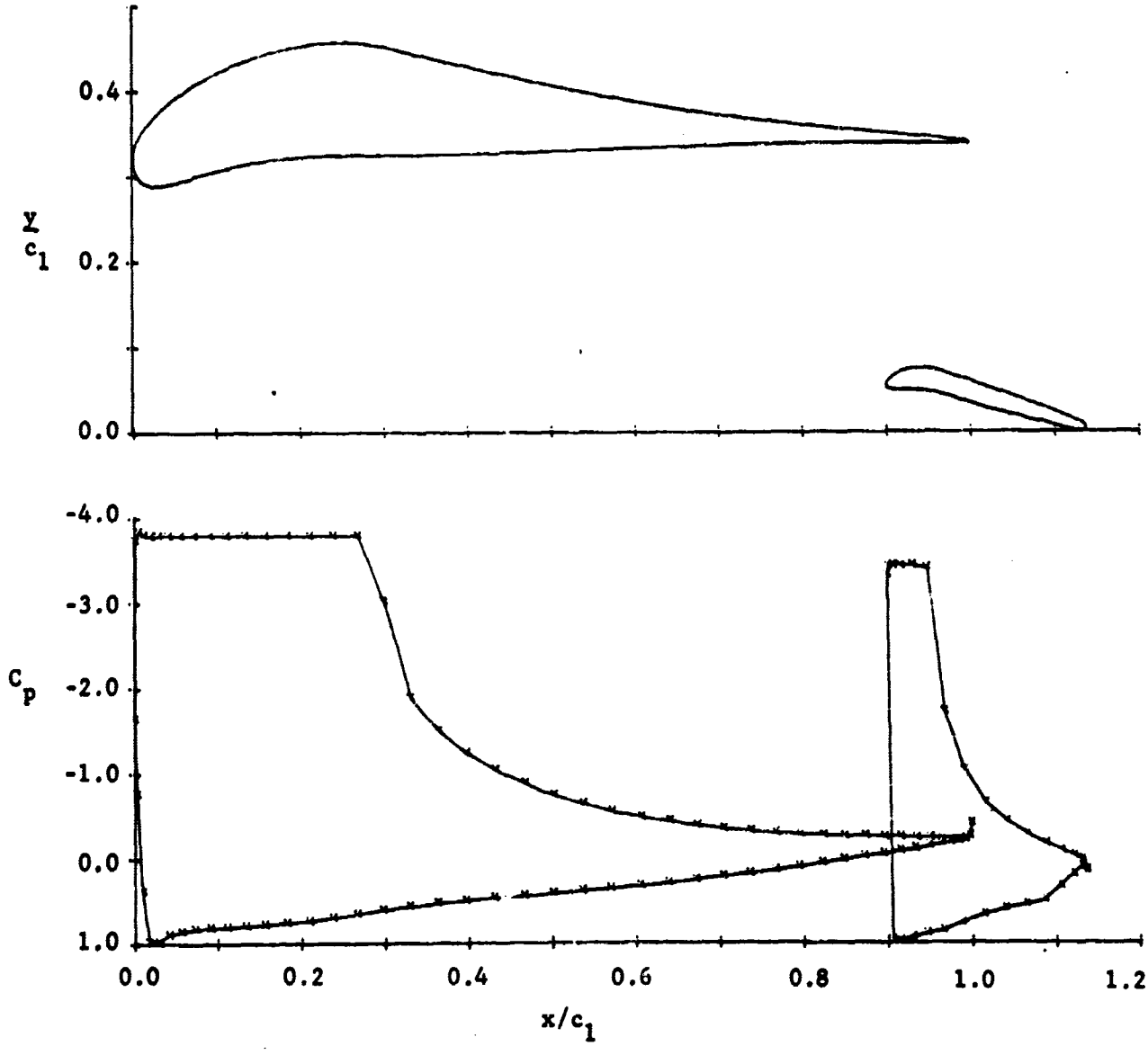

Figure 17. Geometry and pressure distribution of two-element optimum airfoil for $Re_{01} = 10^7$ and $Re_{02} = 2 \times 10^6$, $C_L = 2.45446$.

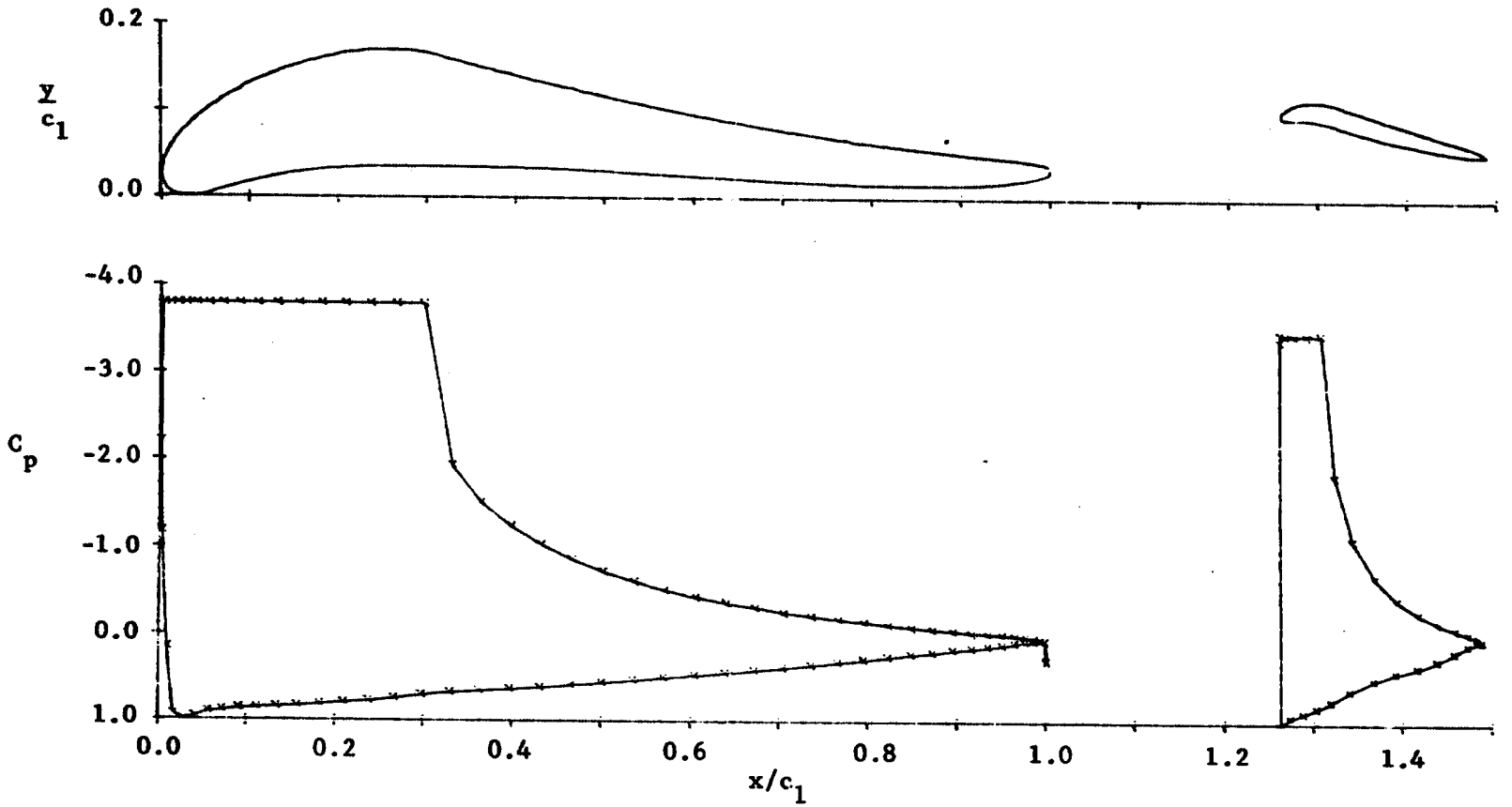

Figure 18. Geometry and pressure distribution of two-element optimum airfoil for $Re_{01} = 10^7$ and $Re_{02} = 2 \times 10^6$, $C_L = 2.50194$.

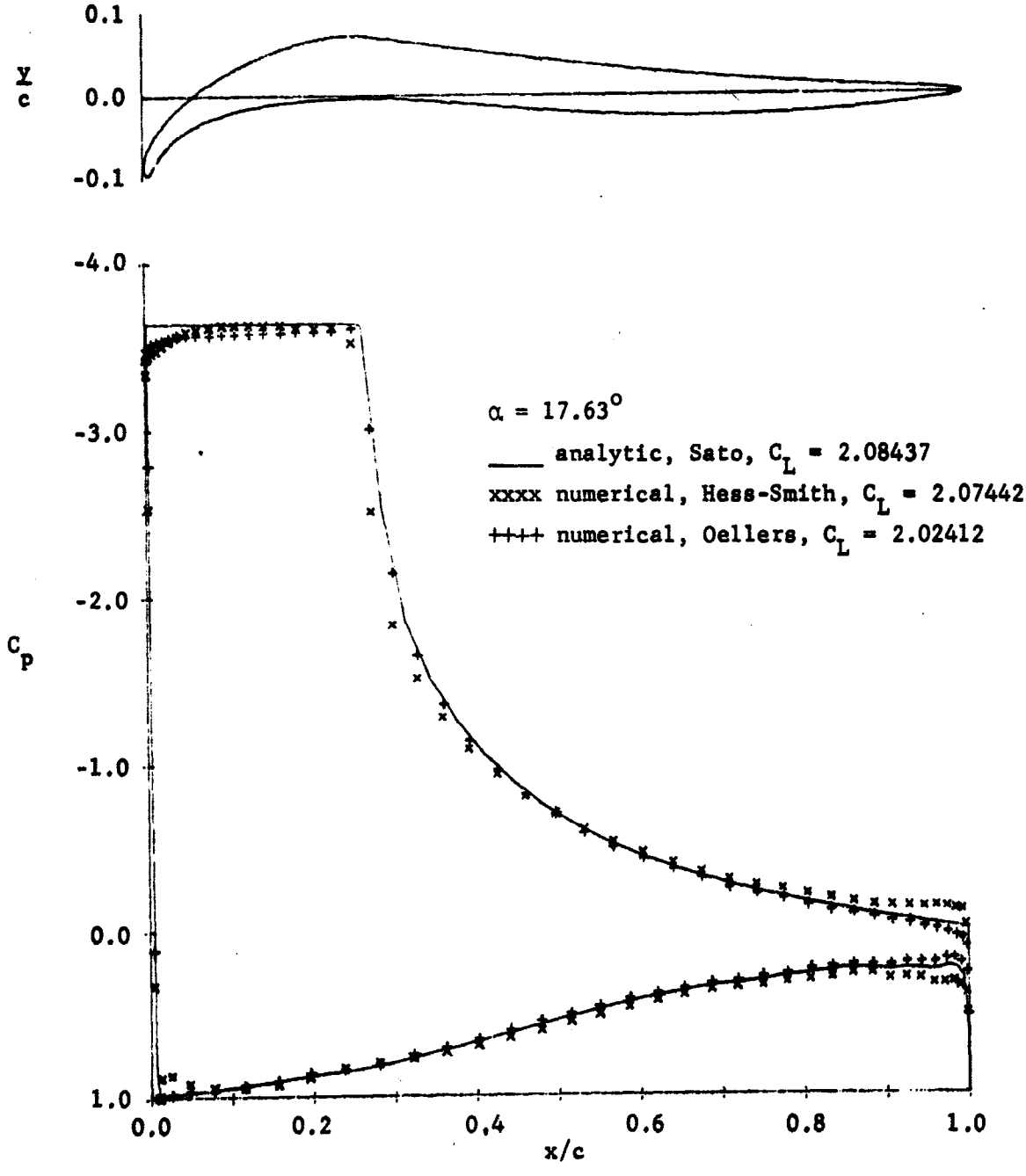

Figure 19. Single-element airfoil designed by Sato's method and pressure distributions computed by three different methods.

pressure distributions. These three pressure distributions were obtained by three different methods and are presented in the same figure for comparison. It can be seen that Oellers' method yields a better result than the one obtained from the Hess-Smith method. Since thick airfoils with blunted leading edges are desirable for practical utilization, modifications in pressure distributions were made, and the new method of airfoil design described in Section III.C was employed to obtain the coordinates. Ninety control points were used and the time consumed by the IBM 360/75 computer was 110 seconds. The resulting geometries and pressure distributions are presented in Figures 20 and 21. Also shown in the figures are the pressure distributions at off-design attitudes, i.e., at angles of attack smaller than the designed values, 17.6° for $Re_0 = 5 \times 10^6$ and 18.6° for $Re_0 = 10^7$.

Because of the different quantities used in computing Reynolds number, the free stream Reynolds number Re_∞ may be obtained from the formula

$$Re_\infty = Re_0 \frac{U_\infty}{U_0} \frac{s_U}{s_0} \frac{c}{s_U}$$

where all the quantities are available from Tables 1, 2 and 3. The value of c/s_U is approximately 0.925 for the examples generated. For wing-flap configurations, the main element is taken as the reference.

Although s_U has been used as the reference length in defining the lift coefficient in Chapter II, the chord length c is commonly used. Hence the C_L values shown in Figures 20 and 21 are based on the chord length and those shown in Figures 9 to 18 are based on the chord length of the main element.

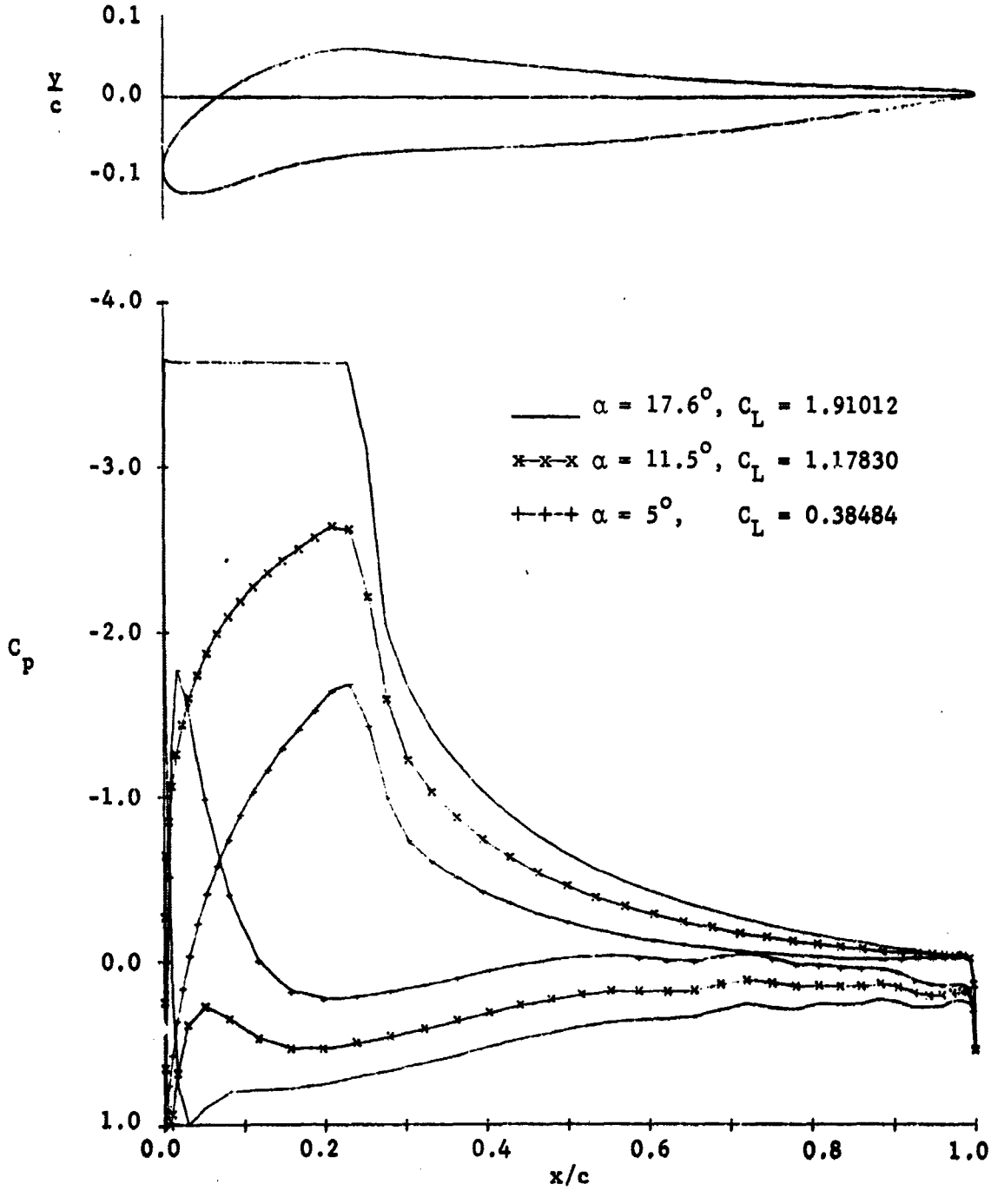

Figure 20. Single-element optimum airfoil for $Re_o = 5 \times 10^6$ and pressure distributions at three different angles of attack.

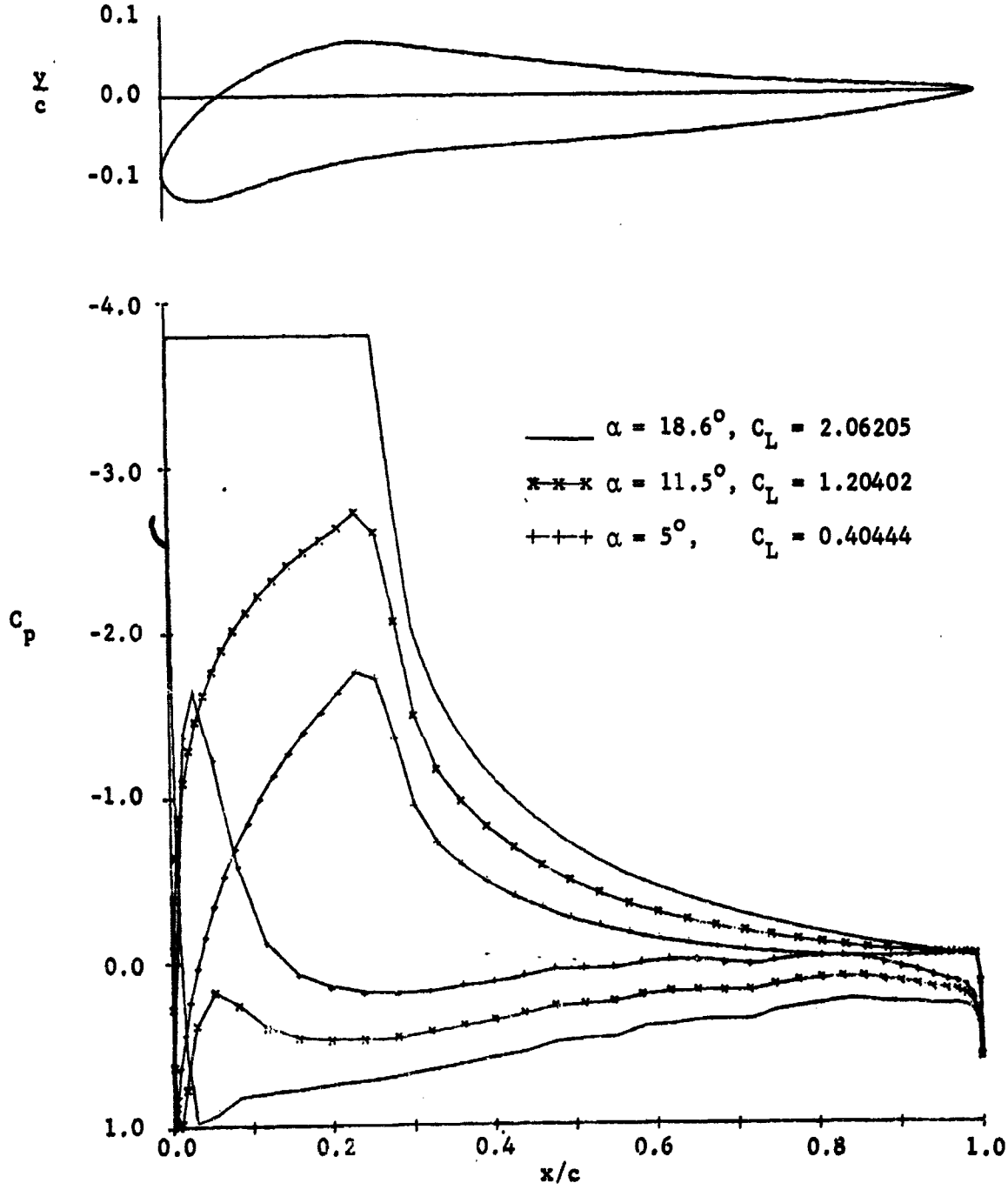

Figure 21. Single-element optimum airfoil for $Re_c = 10^7$ and pressure distributions at three different angles of attack.

V. DISCUSSION AND CONCLUDING REMARKS

A. Single-Element Optimum Airfoils

Although the main interest of this research was to obtain the geometries of multiple-element airfoils optimized for maximum lift coefficient, several single-element airfoils were also generated. Two single-element airfoils with different Reynolds numbers are presented in Figures 20 and 21 together with their pressure distributions. The geometries of these two airfoils are quite similar. This is not surprising since the optimum pressure distributions on the upper surface of each airfoil do not differ very much (see Figure 22). The modified pressure distributions on the lower surface are also similar. The only difference between these airfoils is the attitude at which each airfoil is to be operated. As can be seen in Tables 1, 2 and 3, larger Reynolds numbers always result in higher peak velocity and longer extent of peak velocity plateau. Hence lift coefficient increases as Reynolds number increases. As a consequence, single-element optimum airfoils with larger Reynolds numbers usually operate at higher angles of attack. The geometry is obtained first by Sato's method. The results all possess leading edges of high curvature and the thickness ratios are smaller than 9%. This highly curved leading edge is the consequence of the abrupt pressure drop at the front stagnation point as demanded by optimization of pressure distribution, but it is not suitable for operating the airfoil at other angles of attack. When the airfoil is to be operated at angles of attack smaller than the design value, the front stagnation point moves along the airfoil surface in a clockwise direction. This leads to a small region

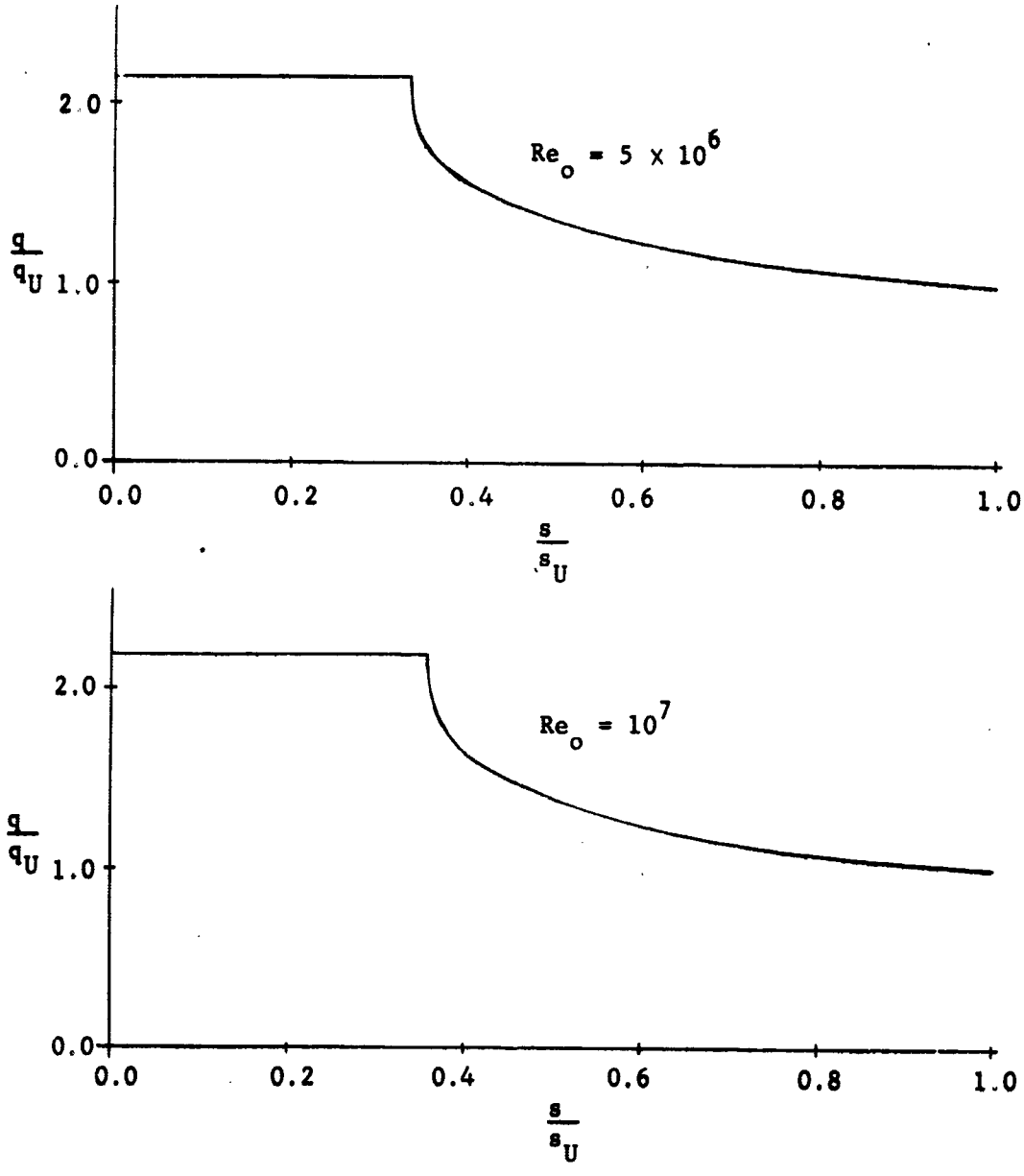

Figure 22. Optimized pressure distribution on the upper surface of a single-element airfoil for two different Reynolds numbers.

of high velocity on the lower surface and consequently a flow separation when the velocity is decreasing toward the trailing edge. Although the flow separation on the lower surface is probably not as extensive as the one on the upper surface, the precise effects are not known. The curvature near the leading edge was reduced by modifying the geometry obtained from Sato's method in an arbitrary manner. This modification not only changed the abrupt pressure drop to a gradual one but also destroyed the optimum pressure distribution which is composed of a plateau and a Stratford zero skin friction pressure distribution. What needs to be done is to modify this modified airfoil in such a way that the gradual pressure drop, as well as the plateau and Stratford's distribution, can be obtained. This modification is accomplished by employing the new method of airfoil design developed in Section III.C. As shown in Figures 20 and 21, each airfoil has a leading edge of small curvature, a moderate thickness (12%) and a not too thin aft part. The pressure distribution on the upper surface does have a plateau and the recovery part does follow the Stratford distribution. But, the pressure drop at the front stagnation point is gradual and the trailing edge velocity is not $q_U = 1$. These facts make the airfoil a non-optimized one. However, in view of the conflict between the optimization requirement and other criteria such as the aerodynamic performance at various angles of attack and structural requirement, the compromise made is an appropriate one.

The behavior of these airfoils at lower angles of attack was also examined. The pressure distributions are shown in Figure 20 and 21. They all possess an almost constant free stream pressure on the lower surface. The acceleration on the upper surface is gradual and the position of peak velocity is fairly close to the mid-chord.

B. Two-Element Optimum Airfoils

The examples presented in Figures 9 to 18 are two-element optimum airfoils with free stream Reynolds numbers in the order of 10^6 to 10^7 Because the intention is to design high lift devices, such as a retractable trailing edge flap, chord ratios of approximately 4 are used. It can be seen that geometries of the main elements differ from those of the single-element airfoils with the same value of Re_0. This difference occurs because the optimum pressure distribution is the same for all airfoils of any number of elements while for multiple-element airfoils the pressure distribution of each element is not entirely determined by its own geometry. The geometries of other elements and the relative position of each element are also involved. These examples have indicated that the relative position of two elements plays an important role in determining the geometry of each element. When two elements are in a conventional wing-flap configuration as shown in Figure 9, the influence of the flap on the main element is to induce an increase of circulation which is composed of a velocity increase on the upper surface and a velocity decrease on the lower surface of the main element. However, in order to produce the same optimized pressure distribution, the single-element airfoil is inclined more to the free stream than the main element of a two-element airfoil is On the other hand, the influence of the main element on the flap is to decrease the circulation about the flap. This is indicated by a decrease of velocity on the upper surface of the flap. Hence the inclination of the flap with respect to the free stream is more than that of a single-element airfoil which produces the same pressure distribution. When the distance between two elements is increased, the interaction becomes weaker.

The consequence is that in addition to the slight geometrical change on each element the main element increases its angle of attack, and the flap decreases its angle of attack. Because the high peak velocity plateau on the upper surface of the flap induces a strong flow field in the neighborhood of the flap's leading edge, low speed near the trailing edge of the main element as required by the optimization can not be realized if the distance between the two element is too small (see Figures 9 and 14). Therefore, from an aerodynamic point of view, some minimum distance must be maintained between the two elements in order that the optimum pressure distribution can be realized by geometrically realistic airfoils. Placing the flap directly beneath the aft part of the main element should be avoided. Under that circumstance, the lower surface of the main element is approximately parallel to the flap and the peak velocity plateau on the flap has a strong induced velocity. The aft part of the main element will contribute negative lift force unless the distance between two elements is made large (see Figures 12 and 17). It may be noticed that the requirement $q_U = 1$ at the trailing edge of the main element is not quite satisfied in most cases. This is attributed to the fact that during the modification of the airfoil geometries, the relative position of two elements in the x direction is kept unchanged. This restricts the freedom of modification because the relative position in the x direction is fixed at its starting value. Therefore, several starting configurations are used and only the one which gives the result of $q_U = 1$ on main element should be retained. An alternative solution would be to change the entire velocity distribution according to the real value of q_U. But, since optimum velocity distribution has been reached over a large portion of

the airfoil surface and a new value of q_U would result in a new value of s_U, the gain of changing the velocity distribution is overshadowed by the trouble it causes. With regard to the starting configuration, the single-element optimum airfoils obtained by a combined use of Sato's method and the new method developed in Section III.C is chosen, although any geometry may be used. The reason for doing so is two-fold. First, all of the single-element optimum airfoils have moderate thicknesses and reasonably blunt leading edges. Second, in this way the time consumed by the computer in modifying the geometries will not be as long as the time which would be consumed by starting from an arbitrary geometry.

C. Remarks About the Design Procedure

When the velocity distribution on the surface of a given airfoil is to be computed by Oellers' method, two sets of points are used. One is the given control points which represent the airfoil. These points are on the airfoil surface. The other set is the set of mid-chord points which are slightly removed from the airfoil surface. The integral equation (28) is applied at the mid-chord points and the control points serve the purpose of constructing the coefficient matrix K_{ij}. Therefore, when the geometry of an airfoil is under modification in order to obtain the optimum pressure distribution, the values of y computed by equation (30) are the ones for the mid-chord points. In order to compute the velocity distribution on the surface of the modified airfoil, a new set of control points must be obtained. Two ways of determining the co-ordinates of control points from the mid-chord points were considered in the early stage of this research but they did not give satisfactory

results. One of these was to take the middle point of the straight line which connects two adjacent mid-chord points to be the control point. The other was to form a polygon such that the new mid-chord points were the middle points of each side and the corners of this polygon were taken to be the new control points. Because the x coordinates of the mid-chord points were kept unchanged during the modification, these two methods gave bad results after a certain number of iterations. It was felt that the means by which mid-chord points were obtained as initiated by Hess and Smith is not appropriate for the purpose of modifying geometries. Between the set of control points and the set of mid-chord points, one is permitted to go only from the former to the latter, but not the reverse. To liberalize this restriction, interpolation would be a desirable tool. In other words, when the control points which represent an airfoil were given, an interpolation was made to give the coordinates of 'mid-chord points' where equation (28) is to be applied. After the new y coordinates of 'mid-chord points' were obtained from equation (30), the new control points were determined by interpolation. A Lagrangian four point interpolation was used and the results were very good. Because none of the interpolation methods gave good results when the slope of the curve formed by the given points was large, certain rotations of coordinate axes were necessary when doing interpolation near the leading edge of an airfoil.

During the modification of airfoil geometries, certain values of V_j are to be used in equation (30) as the desired velocities. Usually, the starting configuration is chosen so that the velocity distribution on the lower surface is approximately a linear acceleration from leading

edge to trailing edge. Hence, those γ_j's which are computed from step (ii) of Section III.C as the velocities on the lower surface may be retained. Only those on the upper surface need to be changed. In generating the examples shown in Figures 20 and 21, it is found that too many restrictions on γ_j's may result in either an unacceptable geometry or a non-converging iterative process. The most severe situation takes place when attempts are made in order to reach the exact optimum velocity distribution near the trailing edge. The action taken to overcome this difficulty is not to pay much attention to the trailing edge. Because the viscous effects have not been taken into consideration in the design process, the airfoils obtained will not generate exactly the desired pressure distribution. This deviation of real pressure distribution from the desired one is especially large near the trailing edge. Hence there is really no need to attempt to reach the exact pressure distribution near the trailing edge. In the case of two-element airfoils, this problem seems to be less severe because geometries which correspond to the desired velocity distributions can always be obtained by appropriate choice of relative position of the elements.

LIST OF REFFRENCES

1. Liebeck, R. H. and Ormsbee, A. I., "Optimization of Airfoils for Maximum Lift," J. of Aircraft, Vol. 7, No. 5, pp. 409-415, Sept./Oct., 1970.

2. Stratford, B. S., "The Prediction of Separation of the Turbulent Boundary Layer," J. of Fluid Mechanics, Vol. 5, pp. 1-16, 1959.

3. Stratford, B. S., "An Experimental Flow With Zero Skin Friction Throughout Its Region of Pressure Rise," J. of Fluid Mechanics, Vol. 5, pp. 17-35, 1959.

4. Sato, J., "An Exact Two-Dimensional Incompressible Potential Flow Theory of Airfoil Design With Specified Velocity Distributions," Trans. Japan Soc. Aero. Space Sci., Vol. 9, No. 14, pp. 11-18, 1966.

5. Lighthill, M. J., "A New Method of Two-Dimensional Aerodynamic Design," Reports and Memoranda No. 2112, Aeronautical Research Committee, London, April, 1945.

6. Weber, J., "The Calculation of the Pressure Distribution on the Surface of Thick Cambered Wings and the Design of Wings With Given Pressure Distribution," Reports and Memoranda No. 3026, Aeronautical Research Committee, London, June, 1955.

7. Garrick, I. E., "Potential Flow About Arbitrary Biplane Wing Sections," NACA Technical Reports, No. 542, 1935.

8. Hess, J. L. and Smith, A. M. O., "Calculation of Potential Flow About Arbitrary Bodies," Progress in Aeronautical Sciences, Vol. 8, pp. 1-138, Pergamon Press, 1967.

9. Martensen, E., "Berechnung der Druckverteilung an Gitterprofilen in ebener Potentialstromung mit einer Fredholmschen Integralgleichung," Archive for Rational Mechanics and Analysis, Vol. 3, No. 3, pp. 235-270, 1959.

10. Jacob, K. ard Riegels, F. W., "Berechnung der Druckverteilung endlich dicker Profile ohne und mit Klappen und Vorflugeln," Zeitschrift fur Flugwissenschaften, Vol. 11, No. 9, pp. 357-367, September, 1963.

11. Oellers, H. J., "Die Inkompressible Potentialstromung in der Ebener Gitterstufe," Jahrbuch 1962 der Wissenschaftlichen Gesellschaft fur Luft- und Raumfahrt e. v., pp. 349-353.

VITA

Allen Wen-shin Chen was born on [redacted] in [redacted] He received his elementary education in Taiwan and graduated from Provincial Tainan First Middle School in 1961. In the same year he entered National Taiwan University to study mechanical engineering. After obtaining a Bachelor of Science degree in mechanical engineering in 1965, he served one year in the Chinese Air Force as a second lieutenant. He was admitted to the Graduate College of the University of Illinois in 1966 and obtained his Master of Science degree in Aeronautical and Astronautical Engineering in 1969 with a thesis entitled "The Supersonic Flow Near the Intersection of Two Wedges." He was employed by the Aeronautical and Astronautical Engineering Department of the University of Illinois from 1967 to 1970 as a teaching assistant. In the spring of 1970, a contract was granted by the Langley Research Center of the National Aeronautical and Space Administration to explore a new method of airfoil design and he has been working as a research assistant since then.